

**REVISITING THE IMPACT OF H₂O₂ ON INTRACELLULAR NRF2 LEVELS
USING A NEWLY DEVELOPED OXYGEN-INDEPENDENT NRF2
BIOSENSOR**

by

SEYED MOHAMMAD MIRI

Submitted to the Graduate School of Engineering and Natural Sciences

in partial fulfilment of

the requirements for the degree of Master of Science

Sabanci University

December 2024

Seyed Mohammad Miri 2025 ©

All Rights Reserve

ABSTRACT

REVISITING THE IMPACT OF H₂O₂ ON INTRACELLULAR NRF2 LEVELS USING A NEWLY DEVELOPED OXYGEN-INDEPENDENT NRF2 BIOSENSOR

SEYED MOHAMMAD MIRI

Molecular Biology, Genetics and Bioengineering, M.Sc. Thesis, October 2024

Thesis Supervisor: Prof. Dr. Selim Çetiner

Thesis Co-supervisor: Dr. Emrah Eroğlu

Keywords: Nrf2, oxygen-insensitive biosensors, hydrogen peroxide (H₂O₂),
chemogenetic tools, Auranofin

Reactive oxygen species (ROS) are central to cellular communication, and Nrf2 serves as a crucial transcription factor in maintaining redox balance. Despite extensive research, the interplay between Nrf2 and hydrogen peroxide (H₂O₂) remains contentious. This study aimed to explore how varying intracellular H₂O₂ concentrations impact Nrf2 activity in brain endothelial cells under physiological oxygen conditions (5 kPa O₂), as opposed to conventional hyperoxic conditions. We developed the Pericellular Oxygen-Insensitive Nrf2 Total LEvel Reporter (POINTER), a novel biosensor for oxygen-independent Nrf2 monitoring in human cerebral microvascular endothelial cells (hCMEC/D3). By utilizing external H₂O₂, chemogenetic production of H₂O₂ via modified D-amino acid oxidase (mDAAO), and Auranofin-induced oxidative stress, we evaluated the effects of H₂O₂ on Nrf2. Our findings demonstrated significantly lower Nrf2 levels under physioxia compared to room air, with Auranofin and chemogenetically produced H₂O₂ showing distinct effects on Nrf2 modulation. POINTER revealed that while Auranofin significantly increased Nrf2 levels under physiological oxygen, exogenous and chemogenetically produced H₂O₂ did not sustain this effect. These results underscore the nuanced regulation of Nrf2 by both antioxidant inhibition and H₂O₂ elevation under physioxic conditions.

ÖZET

YENİ GELİŞTİRİLEN OKSİJEN-BAĞIMSIZ NRF2 BİYOSENSÖRÜ KULLANILARAK H₂O₂'NİN HÜCRE İÇİ NRF2 SEVİYELERİNE ETKİSİNİN YENİDEN İNCELENMESİ

SEYED MOHAMMAD MIRI

Moleküler Biyoloji, Genetik Ve Biyomühendislik, Yüksek Lisans Tezi, Eylül 2024

Tez Danışmanı: Prof. Dr. Selim Çetiner

Tez Eş-danışmanı: Dr. Emrah Eroğlu

Anahtar Kelimeler: Nrf2, oksijenden bağımsız biyosensörler, hidrojen peroksit (H₂O₂),
kemogenetik araçlar, Auranofin

Reaktif oksijen türleri (ROS), hücrel iletişimde merkezi bir rol oynar ve Nrf2, redoks dengesi sağlamak için kilit bir transkripsiyon faktörüdür. Ancak Nrf2 ile hidrojen peroksit (H₂O₂) arasındaki ilişki, kapsamlı araştırmalara rağmen tartışmalı olmaya devam etmektedir. Bu çalışmanın amacı, fizyolojik oksijen koşulları (5 kPa O₂) altında beyin endotel hücrelerinde değişen H₂O₂ seviyelerinin Nrf2 aktivitesini nasıl etkilediğini, tipik hiperoksik koşullarla karşılaştırarak araştırmaktır. Bu amaçla, insan beyin mikrodamar endotel hücrelerinde (hCMEC/D3) oksijenden bağımsız Nrf2 izlemeyi sağlayan Perisellüler Oksijen-Duyarsız Nrf2 Toplam Seviye Göstergesi (POINTER) adlı yenilikçi bir biyosensör geliştirdik. Eksojen H₂O₂ uygulaması, modifiye edilmiş D-amino asit oksidaz (mDAAO) ile kemogenetik H₂O₂ üretimi ve Auranofin ile indüklenen oksidatif stres kullanarak, H₂O₂'nin Nrf2 üzerindeki etkilerini değerlendirdik. Sonuçlarımız, fizyoksia koşullarında Nrf2 seviyelerinin oda havasına göre önemli ölçüde daha düşük olduğunu gösterdi ve Auranofin ile kemogenetik olarak üretilen H₂O₂'nin Nrf2 modülasyonunda farklı etkiler sergilediğini ortaya koydu. POINTER, Auranofin'in fizyolojik oksijen koşullarında Nrf2 seviyelerini anlamlı ölçüde artırdığını, ancak eksojen ve kemogenetik olarak üretilen H₂O₂'nin bu etkiyi sürdürmediğini ortaya çıkardı. Bu sonuçlar, fizyoksik koşullarda Nrf2'nin hem antioksidan inhibisyonu hem de H₂O₂ artışı ile karmaşık bir şekilde düzenlendiğini vurgulamaktadır.

Acknowledgement

First and foremost, I would like to express my sincere gratitude to my advisor, Professor Emrah Erouglu, for his invaluable guidance, continuous support, and unwavering belief in my abilities throughout this research journey. His commitment to fostering intellectual curiosity has had a profound impact on my life. His mentorship has not only honed my research skills but also instilled in me a lifelong passion for learning and discovery. I am truly fortunate to have had the opportunity to work under his tutelage. Wherever I go and in whatever I do, I will always see myself as an EE lab member, carrying the values, experiences, and lessons learned into all future endeavors.

I am deeply indebted to my dear friend, Şeyma, for her unwavering kindness, support, and generosity. She was always there to lend an ear, offer advice, and provide encouragement. Her friendship has been a constant source of strength and inspiration, making this journey infinitely more enjoyable. The kindness she has shown is something I will carry with me throughout my life, and I wish her nothing but the best. Stay wonderful, my friend!

I would like to acknowledge Asal's role in inspiring my initial motivation to join the EE lab and her support along the way. Additionally, I greatly enjoyed our fruitful collaboration during a part of my master's journey.

I am grateful to my other lab mates, Sarah, Merve, Joudi, Sena, Asel, and Melike, for their camaraderie, support, and helpful discussions. Their presence in the lab created a positive and stimulating environment that fostered creativity and collaboration.

I would also like to thank Buşra for her valuable contributions in the early stages of this project, helping to spark the initial idea.

I am also thankful to my family for their emotional and financial support, which has made this journey much more manageable.

Finally, I would like to acknowledge the support of the Scientific and Technological Research Council of Türkiye (TÜBİTAK), whose funding made this research possible.

Dedication page
Lorem ipsum lorem ipsum

TABLE OF CONTENTS

TABLE OF CONTENTS	viii
LIST OF FIGURES	x
LIST OF TABLES	xi
LIST OF SYMBOLS AND ABBREVIATIONS	xii
1. INTRODUCTION	1
1.1. Nrf2: A Comprehensive Overview	1
1.1.1. History	1
1.1.2. Mechanism	1
1.1.3. Structure and Domains of Nrf2	3
1.1.4. Structure and Domains of KEAP1	5
1.1.5. Applications.....	7
1.2. Hydrogen Peroxide (H ₂ O ₂).....	8
1.3. Auranofin.....	11
1.3.1. Measurement of Intracellular H ₂ O ₂	12
1.4. hCMEC and hCMEC/D3.....	15
1.5. Pericellular Oxygen in Physiology and Physiological Studies.....	16
2. AIMS OF THE STUDY	19
3. MATERIALS	20
3.1. Chemicals	20
3.2. Equipments	20
3.3. Molecular Biology Kits	20
3.4. Enzymes	21
4. METHODS	22
4.1. Transformation Protocol.....	23
4.2. Cloning	23
4.3. Plasmid Extraction.....	24

4.4.	Lentivirus production and purification	25
4.5.	Cell Culture	26
4.6.	Imaging Buffer Preparation	27
4.7.	Live-cell Imaging	27
4.8.	Confocal Imaging	28
4.9.	FACS Analysis.....	29
4.10.	Cell Viability Assay.....	30
4.11.	Quantitative (Real-Time) PCR.....	30
4.12.	Data Analysis.....	31
4.13.	Statistical Analysis.....	32
5.	RESULTS	33
5.1.	Principle and Validation of the Oxygen-Independent Biosensor: POINTER	33
5.2.	Assessing POINTER's Functionality in Different Oxygen Conditions	36
5.3.	Investigating the Relationship Between Oxidative Stress and Nrf2 Using Three Approaches to Manipulate H ₂ O ₂ Levels.....	37
5.3.1.	Exogenous Application of H ₂ O ₂	38
5.3.2.	Chemogenetic Production of H ₂ O ₂	40
5.3.3.	Pharmacological Induction of H ₂ O ₂	42
5.4.	Persistent Versus Transient H ₂ O ₂ Responses and Their Impact on Nrf2 Activation.....	44
5.5.	Auranofin, but Not Exogenously Supplied or Chemogenetically Produced H ₂ O ₂ , Significantly Enhances Nrf2 Levels Under Normoxic Conditions	47
6.	DISCUSSION	51
7.	CONCLUSION	56
8.	BIBLIOGRAPHY	57
	APPENDIX A	67
	APPENDIX B	68
	APPENDIX C	69

LIST OF FIGURES

Figure 1.1. The schematic illustration of two states of the Nrf2 pathway. ...	3
Figure 1.2. Structural Domains of Nrf2.	4
Figure 1.3. Structural Domains of Keap1.	6
Figure 1.4. Approaches to Increase Intracellular H ₂ O ₂	10
Figure 1.5. Chemical Structure of Auranofin.	11
Figure 1.6. Mechanism of the HyPer7 Biosensor	14
Figure 1.7. Impact of Oxygen Levels on GFP Fluorescence.	17
Figure 4.1. Schematic representation of main methodology used in this study.....	22
Figure 5.1. Functionality and Application of the POINTER Biosensor.	34
Figure 5.2. FACS diagrams of hCMEC/D3 cells.	35
Figure 5.3. Confocal images of hCMEC/D3 cells	36
Figure 5.4. Real time HyPer7.2 Biosensor Responses	39
Figure 5.5. Dose-response curves of hCMEC/D3	40
Figure 5.6. Chemogenetic Control of H ₂ O ₂	42
Figure 5.8. Auranofin-Induced Elevation of Intracellular H ₂ O ₂	44
Figure 5.9. Clearance of Exogenously Administered H ₂ O ₂	45
Figure 5.10. Sustained H ₂ O ₂ levels.....	46
Figure 5.11. Residual H ₂ O ₂ Levels	47
Figure 5.12. Nrf2 levels to chemogenetic H ₂ O ₂ production.....	48
Figure 5.13. Nrf2 response to exogenous H ₂ O ₂ and Auranofin.	49
Figure 5.14. Comparative Nrf2 activation by different treatments.	50

LIST OF TABLES

Table 4.1: The sequence of ARE, minP, miniGFP, and the primers	24
Table 4.2: List of primers used for real time qPCR.....	31

LIST OF SYMBOLS AND ABBREVIATIONS

α	Alpha
β	Beta
μg	Microgram
μl	Microliter
μM	Micromolar
mM	Millimolar
nM	Nanomolar
ARE	Antioxidant response element
BBB	Blood-brain barrier
bZIP	Basic leucine zipper
BTB	Broad Complex, Tramtrack, and Bric-à-brac
CKD	Chronic kidney disease
CNC	Cap 'n' Collar
cpYFP	Circularly permuted Yellow Fluorescent protein
CTR	C-terminal region
CUL3	Cullin3
DCFH	Dihydrodichlorofluorescein
DGR	Double Glycine Repeat
DMEM	Dulbecco's modified Eagle's medium
FACS	Fluorescence-activated cell sorting
FbFPs	Flavin-based fluorescent proteins
FBS	Fetal bovine serum
FMN	flavin mononucleotide
GFP	Green fluorescent protein
GPx	Glutathione peroxidase
GSH	Glutathione
GSK	Glycogen synthase kinase
GSR	Glutathione reductase
GST	Glutathione S-transferase
H ₂ O ₂	Hydrogen peroxide
HEK	Human embryonic kidney
HO-1	heme oxygenase-1
hCMEC	Human cerebral microvascular endothelial cell
IVR	Intervening region
Keap1	Kelch-like ECH-associated protein 1
LOV	Light, Oxygen, or Voltage
minP	Minimal promoter
mDAAO	Modified D-amino acid oxidase
NADPH	Nicotinamide adenine dinucleotide phosphate
Neh	Nrf2-ECH homology
NES	Nuclear export signal
NLS	Nuclear localization signals
NQO1	NAD(P)H quinone oxidoreductase 1

NRF2	Nuclear factor-erythroid 2 p45-related factor 2
NTR	N-terminal region
OxyR	Hydrogen peroxide-inducible genes activator
PI	Propidium iodide
POINTER	Pericellular Oxygen-Insensitive Nrf2 Total Level Reporter
pTRAF	Plasmid for transcription factor reporter activation based
ROS	Reactive oxygen species
RXR α	Retinoid X receptor alpha
sMaf	Small musculoaponeurotic fibrosarcoma
TrxR	Thioredoxin reductase

1. INTRODUCTION

1.1. Nrf2: A Comprehensive Overview

1.1.1. History

Nuclear factor erythroid 2-related factor 2 (Nrf2) was first identified in the late 1990s as a crucial transcription factor involved in the cellular response to oxidative stress. Initially recognized for its role in activating antioxidant response elements (AREs) in the genome, Nrf2 has since been established as a master regulator of the cellular defense mechanisms against oxidative damage and electrophilic stress (Itoh et al., 1999). Its discovery has significantly advanced the understanding of how cells adapt to oxidative challenges.

1.1.2. Mechanism

Nrf2 functions as a transcription factor that regulates the expression of various cytoprotective genes. Under normal physiological conditions, Nrf2 is sequestered in the cytoplasm by its repressor protein, Kelch-like ECH-associated protein 1 (Keap1). Keap1 facilitates the ubiquitination and subsequent proteasomal degradation of Nrf2, maintaining low levels of this transcription factor in the cell. In response to oxidative

stress or exposure to electrophilic compounds, specific cysteine residues on Keap1 undergo post-translational modifications. This modification leads to the release and stabilization of Nrf2, allowing it to translocate into the nucleus, a process called canonical Nrf2 activation pathway (Figure 1.1) (Silva-Islas and Maldonado, 2018). In the nucleus, Nrf2 binds to AREs located in the promoter regions of its target genes, initiating the transcription of antioxidant proteins, detoxification enzymes, and other protective molecules, such as heme oxygenase-1 (HO-1), glutathione S-transferase (GST), and NAD(P)H quinone oxidoreductase 1 (NQO1) (Qiao et al., 2023; Ruiz et al., 2013). In addition to the well-established canonical mechanism of Nrf2 activation, recent studies have uncovered alternative, non-canonical pathways that lead to the activation of this important transcription factor. The non-canonical activation of Nrf2 is mediated through Keap1-independent mechanisms. The non-canonical activation of Nrf2 is context-dependent and can be influenced by factors such as cell type and disease state. One key non-canonical pathway involves the sequestration of Keap1 by the ubiquitin-binding protein p62 (also known as SQSTM1). Under conditions of autophagic dysfunction, p62 accumulates and binds to Keap1, preventing it from targeting Nrf2 for degradation. This leads to the stabilization and nuclear translocation of Nrf2, resulting in the transcriptional activation of its target genes (Dodson and Zhang, 2017). Post-translational modifications of p62, such as phosphorylation, can enhance its binding affinity for Keap1, further promoting the non-canonical activation of Nrf2 (Dodson and Zhang, 2017). The relevance of this non-canonical pathway has been demonstrated in certain pathologies, including hepatocellular carcinoma and neurodegenerative diseases associated with autophagy dysregulation (Dodson and Zhang, 2017). Another Keap1-independent mechanism involves the direct regulation of Nrf2's transactivation potential. Mild oxidative stress can induce Nrf2 activation in astrocytes through a non-canonical pathway that does not require Keap1 antagonism. Instead, oxidants like H₂O₂ directly target the Neh5 transactivation domain of Nrf2, enhancing its transcriptional activity (Al-Mubarak et al., 2021). While the canonical pathway is well-established, the non-canonical mechanisms are still being actively investigated, and their precise roles in various physiological and pathological conditions are not yet fully understood.

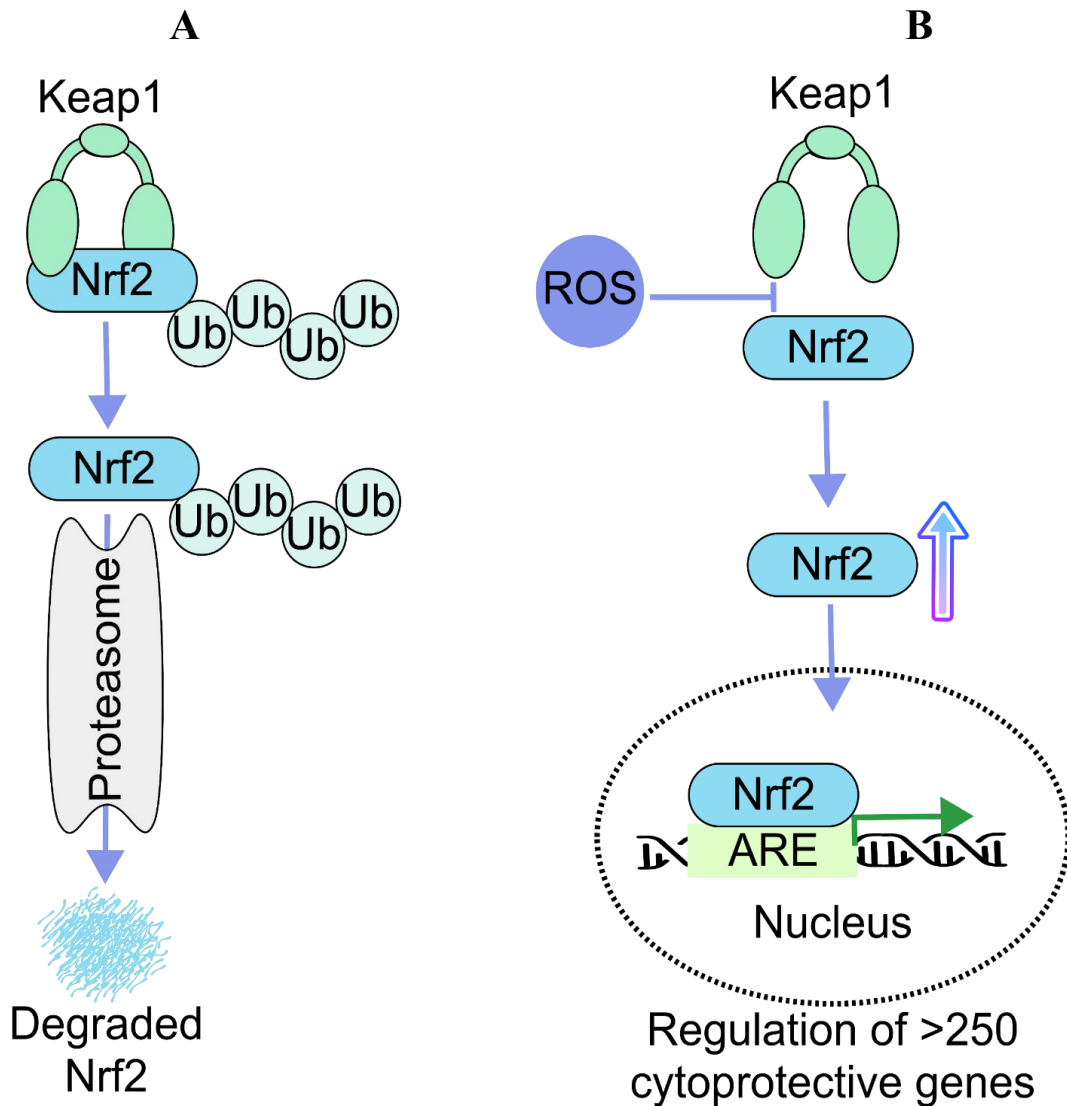


Figure 1.1. The schematic illustration of two states of the Nrf2 pathway. (A) Basal level, where under normal conditions, Nrf2 is bound to Keap1 in the cytoplasm and targeted for proteasomal degradation, maintaining basal low Nrf2 activity. (B) Activated state, where in the presence of ROS, oxidative modifications to Keap1 lead to the release and stabilization of Nrf2. Nrf2 translocates to the nucleus, binds to the antioxidant response element in target gene promoters, and induces the expression of antioxidant and cytoprotective genes, thereby promoting cellular defense against oxidative stress.

1.1.3. Structure and Domains of Nrf2

Nrf2 is a basic leucine zipper (bZIP) transcription factor belonging to the Cap 'n' Collar (CNC) family (Li and Kong, 2009). It consists of 589 amino acids in humans and is

structured into several distinct functional domains, each contributing to its regulatory capabilities (Ma, 2013).

The primary domains of Nrf2 are as follows (Figure 1.2) (Baird et al., 2014; Li and Kong, 2009; Ma, 2013; Robledinos-Antón et al., 2019). Neh2 Domain that is crucial for the interaction with Keap1, the primary repressor of Nrf2. It contains two motifs, the DLG and ETGE motifs, which are essential for binding to Keap1 and regulating Nrf2's stability through ubiquitination. The Neh2 domain also plays a role in the negative regulation of Nrf2 activity, as Keap1 mediates its degradation under basal conditions.

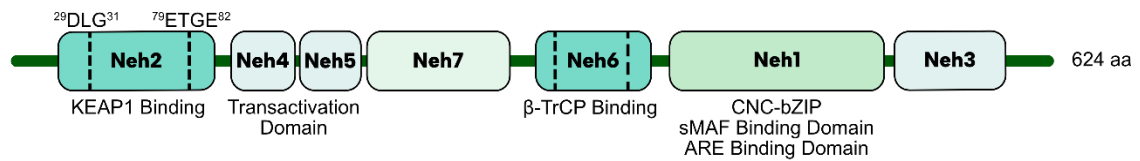


Figure 1.2. Structural Domains of Nrf2. The Neh1 domain is responsible for DNA binding and dimerization with small Maf proteins, allowing Nrf2 to bind to the antioxidant response element (ARE) in target genes. The Neh2 domain mediates interaction with Keap1, which regulates Nrf2 degradation under normal conditions. The Neh3, Neh4, and Neh5 domains are essential for transcriptional activation by recruiting coactivators. The Neh6 domain plays a role in Keap1-independent degradation of Nrf2 through the β -TrCP pathway. Each domain contributes to the regulation of Nrf2 activity and stability in cellular responses to oxidative stress.

Neh1 Domain that contains the bZIP structure necessary for DNA binding and dimerization with small Maf proteins. This domain is critical for the transcriptional activation of Nrf2 target genes, as it facilitates the binding of Nrf2 to AREs in the promoter regions of these genes. Neh3 Domain involved in the transactivation of Nrf2. It interacts with various co-activators, enhancing the transcriptional activity of Nrf2. Neh4 and Neh5 Domains as tandem domains also contribute to the transactivation potential of Nrf2. They interact with transcriptional co-activators and are essential for the full activation of Nrf2 target genes. The Neh6 domain is involved in the negative regulation of Nrf2. It mediates the degradation of Nrf2 through mechanisms independent of Keap1, contributing to the fine-tuning of Nrf2 levels in the cell. Neh7 Domain that has been identified as a region that can bind to retinoid X receptor alpha (RXR α), suggesting a role in the integration of Nrf2 signaling with other nuclear receptor pathways. Neh8

Domain that although less characterized, may also play a role in Nrf2's regulatory functions.

Nrf2 contains multiple nuclear localization signals (NLS) and a nuclear export signal (NES) (Li and Kong, 2009; Ma, 2013). Nrf2 has a bipartite NLS located in the basic region of the Neh1 domain, which is critical for its nuclear import. Additionally, monopartite NLS motifs are present at both the amino-terminus and carboxyl-terminus of Nrf2. The NES is located within the bZIP domain and is responsible for the nuclear export of Nrf2 under basal conditions. This dynamic regulation of Nrf2 localization is essential for its function as a transcription factor. Moreover, Nrf2 contains several conserved cysteine residues that play important roles in its functions. The cysteine residues in Nrf2 can undergo post-translational modifications, which can influence its stability and activity (Tonelli et al., 2018).

1.1.4. Structure and Domains of KEAP1

The KEAP1 protein is a central regulator of the Nrf2 pathway. KEAP1 mediates this regulation by interacting with Nrf2, controlling its stability and degradation under normal conditions. KEAP1 contains several key structural domains that enable its regulatory functions: NTR (N-terminal region), BTB (Broad Complex, Tramtrack, and Bric-à-brac), IVR (Intervening Region), Kelch/DGR (Double Glycine Repeat), and CTR (C-terminal region) (Figure 1.3). Each domain contributes uniquely to the regulation of Nrf2.

The NTR of KEAP1 is involved in regulating the protein's stability and functional interactions. While its role in direct Nrf2 binding is less emphasized compared to other domains, NTR is crucial for ensuring KEAP1's correct folding and localization, enabling it to efficiently interact with other molecular components of the ubiquitin-proteasome system. The BTB domain is essential for KEAP1 homodimerization, a process where two KEAP1 molecules join to form a functional unit. This domain is also responsible for recruiting Cullin3 (CUL3), an E3 ubiquitin ligase complex component, which tags Nrf2 for ubiquitination and degradation. Under normal conditions, KEAP1, through the BTB domain, binds to Nrf2 and keeps its levels low by targeting it for continuous degradation.

This ensures that Nrf2 does not accumulate unnecessarily, maintaining cellular homeostasis.

The IVR of KEAP1 contains multiple cysteine residues that act as redox sensors. This region is particularly responsive to oxidative and electrophilic stress. Upon exposure to reactive oxygen species (ROS) or electrophiles, cysteine residues in the IVR are modified. These modifications induce a conformational change in KEAP1, reducing its ability to bind Nrf2. As a result, Nrf2 escapes degradation and translocates into the nucleus.

The Kelch/DGR domain is one of the most crucial regions for the direct interaction between KEAP1 and Nrf2. This domain binds to the Neh2 domain of Nrf2, specifically targeting its ETGE and DLG motifs. Under normal conditions, this strong interaction ensures that Nrf2 is bound and degraded, preventing the activation of its target genes. However, once the IVR senses oxidative stress, the interaction between the Kelch domain and Nrf2 weakens, allowing Nrf2 to accumulate and exert its protective effects on the cell.

Finally, the C-terminal region (CTR) of KEAP1 is believed to play a role in maintaining the structural integrity of the protein and potentially influencing its overall activity and interaction with other cellular components. Although its function is not as well understood as other domains, the CTR may contribute to the fine-tuning of KEAP1's regulatory capacity.

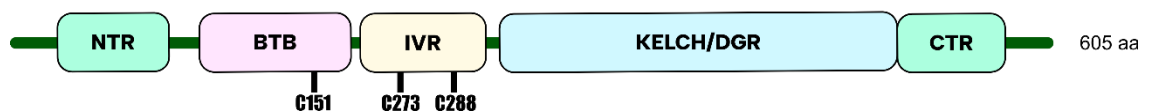


Figure 1.3. Structural Domains of Keap1. The N-terminal BTB domain is responsible for homodimerization and interaction with Cullin3, which is essential for the ubiquitination and degradation of Nrf2. The IVR domain connects the BTB and Kelch domains and regulates the conformation of Keap1. The **Kelch domain** (also known as the DGR domain) contains six repeats and binds to the Neh2 domain of Nrf2, facilitating its degradation under basal conditions. The **CTR** contributes to the overall structure and function of Keap1.

1.1.5. Applications

Nrf2 has emerged as a therapeutic target in various diseases due to its protective roles. Activation of Nrf2 can offer protection against neurodegenerative diseases, cancer, cardiovascular diseases, and conditions associated with oxidative stress. Nrf2 activation has been linked to neuroprotective effects in models of neurodegenerative diseases such as Alzheimer's and Parkinson's disease. By enhancing the expression of antioxidant enzymes, Nrf2 can mitigate oxidative stress and inflammation in neuronal cells, potentially slowing disease progression (Cuadrado, 2016; Saha et al., 2022). Nrf2 is implicated in cardiovascular health, where it protects against ischemia-reperfusion injury and atherosclerosis. Activation of Nrf2 can improve endothelial function and reduce vascular inflammation, offering therapeutic potential in cardiovascular diseases (Chen et al., 2015; Howden, 2013). Nrf2 plays a significant role in metabolic syndrome and diabetes. Its activation can improve insulin sensitivity and regulate lipid metabolism, making it a potential target for the treatment of metabolic disorders (Liu et al., 2021; Matzinger et al., 2018; Seo and Lee, 2013).

Several pharmacological agents that activate the Nrf2 pathway are under investigation, including natural compounds like curcumin and sulforaphane, as well as synthetic drugs. These agents aim to harness Nrf2's protective effects against oxidative stress-related diseases (Calabrese and Kozumbo, 2021; Kwak and Kensler, 2010; Shen et al., 2015). Nrf2 is also associated with the aging process, where its activation may promote longevity by enhancing cellular defense mechanisms against oxidative damage. Research is ongoing to explore Nrf2 activators as potential anti-aging therapies (Bruns et al., 2015; Lewis et al., 2010; Sykiotis and Bohmann, 2008). However, chronic activation of Nrf2, particularly in some cancers, may promote tumorigenesis by enhancing cell survival and proliferation, indicating a dual role in health and disease (Qiao *et al.*, 2023; Ruiz *et al.*, 2013).

Nrf2 is closely linked to the regulation of ROS, particularly hydrogen peroxide (H₂O₂). ROS are byproducts of cellular metabolism and can act as signaling molecules or contribute to oxidative stress. Nrf2 activation is a key adaptive response to elevated ROS levels. When oxidative stress occurs, such as with increased H₂O₂, Nrf2 induces the expression of antioxidant genes that help mitigate oxidative damage by eliminating

excess ROS (Qiao *et al.*, 2023). Furthermore, Nrf2 is involved in maintaining mitochondrial function and biogenesis, ensuring that cells can meet energy demands while managing oxidative challenges (Qiao *et al.*, 2023).

Research has shown that Nrf2 signaling is activated during exercise, which enhances the expression of antioxidant enzymes like catalase. This response is crucial for maintaining redox balance during physical stress (Gallego-Selles *et al.*, 2020). In another study, amino acids have been identified as potential activators of Nrf2. Certain amino acids can modulate the KEAP1-Nrf2 interaction, leading to increased expression of antioxidant enzymes and providing cellular protection against oxidative stress (Egbujor *et al.*, 2024).

Studies indicate that Nrf2 activity is impaired in models of Chronic Kidney Disease (CKD), even in the presence of oxidative stress. This impairment is associated with increased levels of KEAP1, which inhibits Nrf2 activation and contributes to the progression of renal damage (Ruiz *et al.*, 2013).

1.2. Hydrogen Peroxide (H₂O₂)

H₂O₂ is a simple peroxide and a potent oxidizing agent that plays significant roles in both physiological and pathological processes. Its dual nature is evident in its function as a signaling molecule in low concentrations (oxidative eustress) and as a damaging agent at higher concentrations (oxidative distress). H₂O₂ is a ROS that can be produced endogenously through various metabolic pathways. It serves as a central redox signaling molecule, influencing cellular processes such as apoptosis, inflammation, and immune responses. At physiological levels, H₂O₂ can act as a signaling molecule that promotes adaptive responses in cells, a phenomenon referred to as oxidative eustress. This involves the activation of transcription factors like Nrf2 and NF-κB, which help in regulating antioxidant responses and cellular repair mechanisms (Sies, 2017; Zenin *et al.*, 2022). Conversely, when present in supraphysiological concentrations (greater than 100 nM), H₂O₂ can lead to oxidative distress, characterized by damage to cellular macromolecules including lipids, proteins, and nucleic acids. This oxidative damage is primarily mediated

through the generation of highly reactive hydroxyl radicals via Fenton reactions, which can initiate a cascade of cellular damage and contribute to various diseases, including neurodegenerative disorders and cancer (Ransy et al., 2020; Sies, 2017).

Manipulating intracellular H₂O₂ levels is crucial for understanding its roles in cellular signaling and oxidative stress. Various approaches have been developed to achieve this, including exogenous addition, chemogenetic methods, and pharmacological interventions (Figure 1.4).

Exogenous manipulation involves the direct addition of H₂O₂ to the culture medium. This approach allows researchers to elevate intracellular H₂O₂ levels rapidly. Studies have shown that the addition of extracellular H₂O₂ can trigger immediate cellular responses, such as activation of signaling pathways and changes in gene expression. For instance, the effects of exogenous H₂O₂ on endothelial cells have been examined, highlighting its role in modulating phosphorylation pathways critical for cellular function (Saravi et al., 2020).

Chemogenetic approaches provide a more refined means of manipulating H₂O₂ production within cells. One notable method involves the use of D-amino acid oxidase (DAAO) from *Rhodotorula gracilis*, which generates H₂O₂ in the presence of its substrate, D-alanine. By expressing DAAO in specific cell types and targeting it to particular cellular compartments, we can control the spatial and temporal production of H₂O₂. This method has been validated through live-cell imaging techniques that allow real-time monitoring of H₂O₂ levels using genetically encoded biosensors, such as the HyPer sensor (Alim et al., 2014; Saravi *et al.*, 2020; Smolyarova et al., 2022). The manipulation of H₂O₂ has been shown to elicit distinct cellular responses based on the source of H₂O₂ (endogenous vs. exogenous), which can significantly affect signaling pathways related to cell survival and apoptosis (Saravi *et al.*, 2020).

Pharmacological approaches to manipulate H_2O_2 levels often involve the use of compounds that either enhance the production of H_2O_2 or inhibit its degradation. For example, certain drugs can increase mitochondrial ROS production, leading to elevated H_2O_2 levels (Aon et al., 2012). Additionally, antioxidants can be used to modulate H_2O_2 levels by reducing its concentration and mitigating oxidative stress (Drechsel and Patel, 2010). This dual approach allows researchers to study the effects of H_2O_2 in both physiological and pathological contexts, providing insights into its role in diseases such as cancer and neurodegeneration. As an example, recent studies have revealed the potential of Auranofin to increase intracellular H_2O_2 levels (Karsa et al., 2021). Moreover, Compounds that inhibit enzymes responsible for H_2O_2 degradation, such as catalase and peroxidases, can also be used to manipulate intracellular H_2O_2 levels (Thomasz et al., 2007). By preventing the breakdown of H_2O_2 , these inhibitors can enhance its availability, allowing researchers to study its signaling properties more effectively.

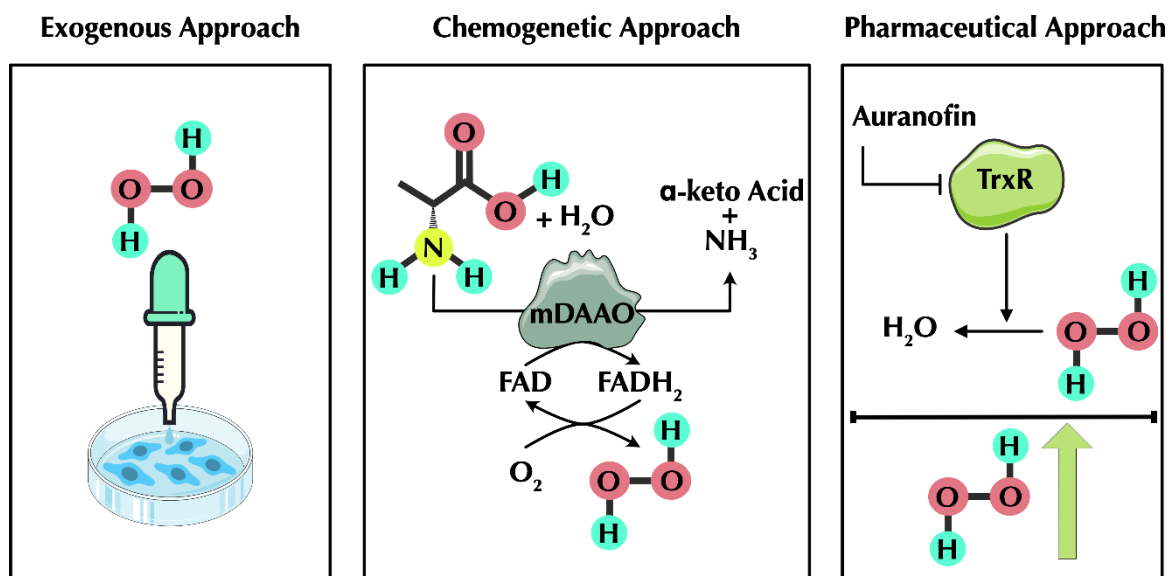


Figure 1.4. Approaches to Increase Intracellular H_2O_2 Levels. (A) Exogenous H_2O_2 addition: H_2O_2 is applied externally to cells, leading to its diffusion across the membrane and raising intracellular H_2O_2 levels. (B) Chemogenetic approach using DAAO: Cells are engineered to express DAAO, which converts D-alanine into H_2O_2 . Upon the addition of D-alanine, this enzymatic reaction increases H_2O_2 production within cells. (C) Pharmaceutical approach using Auranofin: Auranofin, an inhibitor of thioredoxin reductase, reduces the cellular antioxidant capacity, leading to the accumulation of endogenous H_2O_2 .

1.3. Auranofin

Auranofin is a gold-based compound originally developed for the treatment of rheumatoid arthritis (Finkelstein *et al.*, 1976). The development of auranofin dates back to the 1970s when researchers were looking for less toxic alternatives to existing gold therapies for rheumatoid arthritis (Finkelstein *et al.*, 1976). Early studies indicated that the thiol-based ligands in auranofin helped increase its therapeutic index compared to earlier gold compounds (Omata *et al.*, 2006). It was first approved for medical use in 1985 (Finkelstein *et al.*, 1976). Its pharmacological properties extend beyond anti-rheumatic effects, showing promise in various therapeutic areas, including antibacterial, antiviral, antifungal, antiparasitic, and anticancer activities (Gamberi *et al.*, 2022). Its chemical structure features a central gold atom coordinated to a triethylphosphine ligand and a sugar-like structure derived from thiosugar (2,3,4,6-tetra-O-acetyl-1-thio- β -D-glucopyranose) (Caltabiano *et al.*, 1988). This coordination of the gold atom in a linear geometry is crucial for its biological activity. The gold atom in auranofin is in the +1 oxidation state, making it more stable than other gold compounds used historically in medicine, such as sodium aurothiomalate and aurothioglucose (Furst, 1983). These earlier gold drugs had significant side effects due to poor bioavailability and instability, whereas auranofin was developed to mitigate these problems by improving oral absorption and reducing toxicity (Onodera *et al.*, 2019).

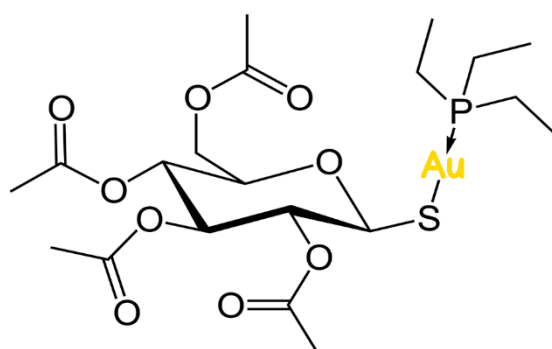


Figure 1.5. Chemical Structure of Auranofin. The figure shows the molecular structure of Auranofin, a gold-based compound featuring a central gold atom bonded to triethylphosphine and a thiosugar ligand. This structure allows Auranofin to inhibit thioredoxin reductase, leading to increased intracellular oxidative stress.

Chemically, auranofin's activity in treating rheumatoid arthritis is linked to its ability to inhibit various cellular processes involved in inflammation. One key mechanism is the inhibition of the enzyme thioredoxin reductase (TrxR), which plays a role in maintaining the redox balance in cells (Becker et al., 2000). By inhibiting this enzyme, auranofin disrupts cellular antioxidant defenses, particularly in immune cells, thus reducing inflammation (Onodera *et al.*, 2019). Additionally, auranofin is known to interfere with mitochondrial function and modulate other redox-sensitive processes, which contribute to its anti-inflammatory effects (Han et al., 2019).

Recent studies have expanded auranofin's potential use beyond rheumatoid arthritis. Its inhibition of thioredoxin reductase has sparked interest in its application as an anti-cancer agent and in the treatment of parasitic diseases such as amebiasis (Abdalbari and Telleria, 2021). Researchers are also exploring its effects in modulating oxidative stress-related pathways, making it a candidate for repurposing in various diseases where redox homeostasis is dysregulated (Tirtorahardjo et al., 2021).

Auranofin primarily functions as a TrxR inhibitor. Thioredoxin reductase is an enzyme involved in maintaining cellular redox homeostasis by regulating the levels of ROS and antioxidants. By inhibiting TrxR, auranofin disrupts the balance of redox state within cells, leading to increased oxidative stress and accumulation of ROS, including H₂O₂ (Cox et al., 2008). This mechanism is believed to contribute to its anticancer effects, as cancer cells often have altered redox states and are more susceptible to oxidative damage (Onodera *et al.*, 2019). Additionally, auranofin has been shown to inhibit various biosynthetic pathways in bacteria, particularly in *Staphylococcus aureus*. It affects cell wall synthesis, DNA replication, and protein synthesis, which makes it a candidate for repurposing as an antibacterial agent, especially against drug-resistant strains like MRSA (methicillin-resistant *Staphylococcus aureus*) (Thangamani et al., 2017; Yu et al., 2022).

1.3.1. Measurement of Intracellular H₂O₂

Measuring intracellular H₂O₂ levels is crucial for understanding its role in various biological processes, including signaling and oxidative stress. Several methods have been developed to quantify H₂O₂ in live cells, each with its advantages and limitations. One

of the most widely used techniques is the fluorescent probe method, which employs genetically encoded sensors like HyPer or its newer version, HyPer 7.2. These biosensors utilize a ratiometric approach, allowing for real-time monitoring of H₂O₂ levels by measuring fluorescence changes in response to oxidation (Jacobs et al., 2022). The advantage of this method is its high sensitivity and specificity, enabling scientists to detect low concentrations of H₂O₂ in physiological conditions (Lyublinskaya and Antunes, 2019). Additionally, there are chemical probes such as dichlorodihydrofluorescein (DCFH) and Amplex Red, which react with H₂O₂ to produce a fluorescent signal, although these methods can sometimes suffer from interference by other reactive species (Bozem et al., 2018; Rhee et al., 2010). Another approach involves electrochemical sensors, which provide real-time measurements of H₂O₂ levels through oxidation-reduction reactions. These sensors can be highly sensitive and allow for continuous monitoring in dynamic biological systems (Ahmad et al., 2022). Mass spectrometry is also employed for H₂O₂ detection, offering high specificity and sensitivity; however, it typically requires more complex sample preparation and is less suitable for real-time measurements (Cochemé et al., 2011). Chemiluminescence is another method that detects H₂O₂ based on its ability to enhance luminescence in certain reactions, providing a sensitive and rapid means of quantification (Wymann et al., 1987). Each of these methods has its own set of challenges, including potential interference from other cellular components, the need for specialized equipment, and varying degrees of complexity in experimental design.

The HyPer 7.2 biosensor is indeed based on circularly permuted yellow fluorescent protein (cpYFP). This design integrates cpYFP into the OxyR regulatory domain from *Neisseria meningitidis*, which enhances its sensitivity and functionality for detecting H₂O₂ in living cells. HyPer 7.2 exhibits two excitation maxima at 400 nm and 499 nm, with a single emission peak at 516 nm, allowing for effective ratiometric measurements of H₂O₂ levels (Pak et al., 2020). The advancements in HyPer 7.2 include improved brightness—approximately 15 to 17 times brighter than earlier versions—and enhanced pH stability, making it suitable for various biological applications without interference from pH fluctuations. This combination of properties positions HyPer 7.2 as a powerful tool for real-time imaging of H₂O₂ dynamics in cellular processes (Pak *et al.*, 2020; Smolyarova *et al.*, 2022).

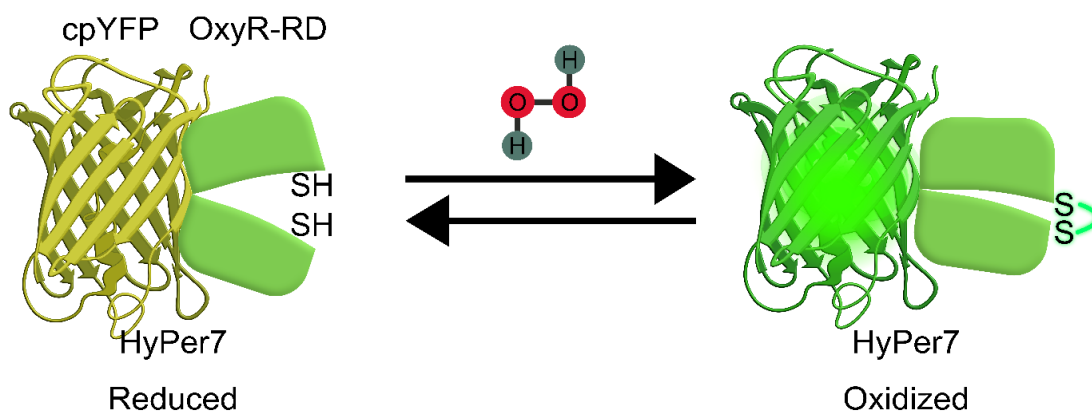


Figure 1.6. Mechanism of the HyPer7 Biosensor. HyPer7 consists of a circularly permuted yellow fluorescent protein fused to the H_2O_2 -sensitive regulatory domain of the bacterial protein OxyR. Upon exposure to H_2O_2 , OxyR undergoes a conformational change that alters the fluorescence of cpYFP, leading to an increase in fluorescence intensity proportional to the levels of H_2O_2 . This real-time, reversible response allows for dynamic monitoring of intracellular H_2O_2 levels with high sensitivity and specificity.

HyPer 7.2 has been utilized in numerous applications, including studies of cell migration, mitochondrial function, and the role of oxidative stress in diseases such as cancer and neurodegenerative disorders. Its ability to provide quantitative measurements of H_2O_2 dynamics in live cells enables researchers to explore the physiological functions of ROS and their implications for cellular signaling pathways (Pak *et al.*, 2020). The biosensor's design allows for targeted expression in specific cell types, enhancing its utility in complex biological systems. The HyPer 7.2 biosensor offers several advantages over traditional methods for measuring intracellular H_2O_2 in live cell imaging. One significant benefit is its ratiometric measurement capability, which utilizes two excitation wavelengths and one excitation wavelength to provide a more accurate quantification of H_2O_2 levels by compensating for variations in probe concentration and environmental factors such as pH and light scattering. This self-calibration feature enhances the reliability of the data, allowing to obtain more precise measurements in dynamic biological systems (Kritsiligkou *et al.*, 2021; Pak *et al.*, 2020). Additionally, being genetically encoded, HyPer 7.2 can be targeted to specific cellular compartments, enabling localized measurements of H_2O_2 and providing insights into its spatial dynamics within the cell (Smolyarova *et al.*, 2022). In contrast to chemical probes, which may suffer from interference by other reactive species, HyPer 7.2 provides a more specific

and sensitive detection of H₂O₂, making it particularly valuable for studying physiological processes where H₂O₂ acts as a signaling molecule. Overall, the combination of high sensitivity, specificity, and the ability to monitor H₂O₂ in real time in living cells positions HyPer 7.2 as a powerful tool for advancing our understanding of redox biology.

1.4. hCMEC and hCMEC/D3

Human cerebral microvascular endothelial cells (hCMEC) are a type of endothelial cell that lines the microvasculature of the brain. These cells play a crucial role in maintaining the blood-brain barrier (BBB), which is essential for protecting the brain from harmful substances and regulating the transport of nutrients and waste products. The hCMEC/D3 cell line is a widely used model for studying the BBB. Developed in 2005, this cell line has become a crucial tool in cerebrovascular research, particularly for understanding drug transport and pathological mechanisms relevant to the central nervous system (CNS). The hCMEC/D3 cell line was developed by transducing normal human brain endothelial cells with lentiviral vectors incorporating human telomerase or SV40 T antigen. This resulted in a stable, immortalized cell line that maintains normal endothelial markers and exhibits blood-brain barrier characteristics, such as tight junctional proteins and the ability to exclude drugs (Weksler et al., 2013; Weksler et al., 2005). The cell line shows robust proliferation, forms capillary tubes in matrix, and maintains a stable karyotype without phenotypic dedifferentiation (Weksler *et al.*, 2005).

The hCMEC/D3 cell line is extensively used to study drug permeability and transport mechanisms at the BBB. It expresses various drug transporters (e.g., ABCB1, ABCG2) and has been used to measure the permeability of different compounds, making it a valuable tool for drug screening (Carl et al., 2010; Poller et al., 2008). This cell line is also used to investigate the responses of brain endothelium to inflammatory and infectious stimuli, as well as interactions with lymphocytes or tumor cells (Weksler *et al.*, 2005). hCMEC/D3 has been utilized to study the expression and function of various

transporters and receptors, providing insights into the molecular mechanisms governing BBB function (Carl *et al.*, 2010; Poller *et al.*, 2008).

Despite its widespread use, the hCMEC/D3 cell line has limitations, particularly in terms of barrier integrity. Studies have shown that it exhibits low transendothelial electrical resistance (TEER) and high permeability to small molecules, which may limit its utility in certain drug permeability studies (Hinkel *et al.*, 2019). Efforts to improve barrier functionality through different culture conditions, supplements, and co-cultures have not significantly enhanced its barrier properties, indicating the need for further optimization or alternative models (Hinkel *et al.*, 2019).

1.5. Pericellular Oxygen in Physiology and Physiological Studies

Pericellular oxygen concentration is a critical factor in cellular physiology, influencing various cellular processes and responses. Understanding and accurately measuring pericellular oxygen levels is essential for physiological studies to ensure experimental conditions closely mimic *in vivo* environments. Pericellular oxygen levels regulate mitochondrial energy metabolism, cell differentiation, and growth. Hypoxia can alter adipokine secretion and is linked to metabolic disorders like type 2 diabetes (Weizenstein *et al.*, 2016; Zachar *et al.*, 2011). Oxygen gradients between extracellular and intracellular compartments influence gene expression, cell fate, and metabolic pathways, including the activity of prolyl hydroxylases and adaptive responses to hypoxia (Dmitriev *et al.*, 2012). Standard cell culture techniques often fail to replicate *in vivo* oxygen dynamics due to limited diffusion through culture media, leading to inaccurate pericellular oxygen levels. This can significantly affect experimental outcomes and reproducibility (Martinez *et al.*, 2019; Pavlacky and Polak, 2020). Novel *in vitro* systems using oxygen-permeable membranes and hypoxic chambers can better control pericellular oxygen levels, providing more physiologically relevant conditions for studying cellular behavior under hypoxia (Martinez *et al.*, 2019). Hypoxia triggers

the activation of HIF pathways, which regulate the expression of numerous genes involved in cellular adaptation to low oxygen conditions. This includes genes related to angiogenesis, metabolism, and survival (Ebbesen et al., 2004). The activity of HIF is modulated by oxygen-dependent enzymes, such as prolyl hydroxylases, which degrade HIF under normoxic conditions but allow its accumulation and activity under hypoxia (Ebbesen *et al.*, 2004). Accurate control and measurement of pericellular oxygen levels are essential for creating *in vitro* models that mimic tissue oxygenation *in vivo*. This is particularly important for studying hypoxia-related physiological and pathological processes (Chen et al., 2013; Pavlacky and Polak, 2020). Variability in pericellular oxygen levels can affect cellular production of ROS, such as hydrogen peroxide, which plays a role in signal transduction and cellular stress responses (Maddalena et al., 2017).

Pericellular oxygen levels can significantly influence the maturation and fluorescence of certain fluorescent proteins. This is particularly relevant in studies conducted under low oxygen conditions, where the fluorescence signal may be affected, potentially impacting the interpretation of experimental results.

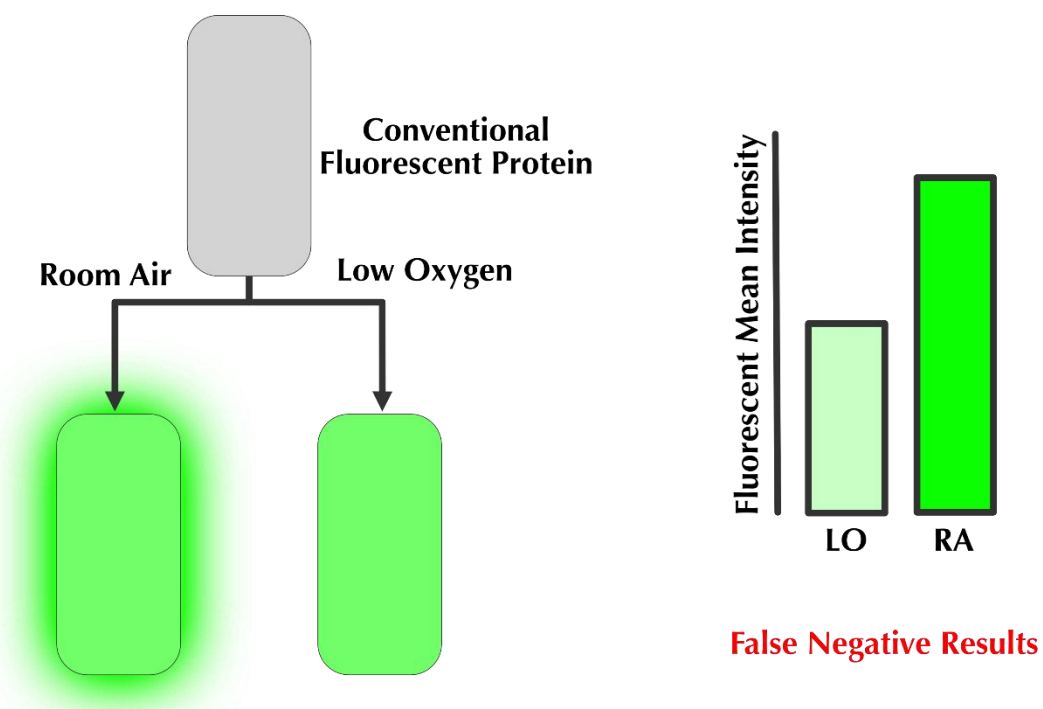


Figure 1.7. Impact of Oxygen Levels on GFP Fluorescence. The figure demonstrates that conventional fluorescent proteins, such as GFP, produce false-negative results under low oxygen conditions (5 kPa O₂). GFP requires oxygen for chromophore maturation, and at low O₂ levels, its fluorescence is significantly reduced, leading to unreliable detection of protein expression. In contrast, under high oxygen conditions,

such as room air (18 kPa O₂), GFP fluorescence is robust, accurately reflecting protein expression.

As an example, green fluorescent protein (GFP) requires oxygen for fluorophore development. In *Streptococcus gordonii*, GFP fluorescence was observed at 0.1 ppm dissolved oxygen but not at 0.025 ppm, indicating a critical threshold for oxygen concentration below which fluorescence does not occur (Hansen et al., 2001). Fluorescent proteins can recover their fluorescence upon reoxygenation. For instance, mKO2 and mAG in HeLa cells showed fluorescence recovery after reoxygenation, with mKO2 exhibiting slower recovery kinetics compared to mAG (Kaida and Miura, 2012). In *S. gordonii*, GFP fluorescence was detected within minutes after shifting from anaerobic to aerobic conditions, indicating rapid fluorophore maturation upon reoxygenation (Hansen *et al.*, 2001). Oxygen itself also can quench the fluorescence of proteins by collisional interactions, which can provide insights into the structural dynamics of proteins. This quenching effect is influenced by the diffusion rate of oxygen through the protein matrix, which is slower than in water (Lakowicz and Weber, 1973).

The good candidates to replace oxygen-based fluorescent proteins are those that do not require oxygen for chromophore maturation, such as those belonging to the Light, Oxygen, or Voltage (LOV) family. These proteins utilize flavins, such as flavin mononucleotide (FMN), as their chromophore and fluoresce efficiently under anaerobic or hypoxic conditions. Recent advancements in LOV-based fluorescent proteins, like miniGFP1 and miniGFP2, have shown promise for live-cell imaging under low-oxygen environments. These proteins are notable for their cyan-green fluorescence and ability to bind flavins selectively, making them useful for biological studies under challenging conditions such as hypoxia (Liang et al., 2022).

Flavin-based fluorescent proteins (FbFPs) are also gaining traction due to their small size, rapid folding, and stability across various pH levels. Notably, proteins such as CreiLOV and variants derived from bacteria like *Pseudomonas putida* have been engineered for enhanced brightness and quantum yield. These mutations have led to significant improvements in their photophysical properties, making FbFPs reliable for applications like fluorescence-based biosensors and real-time imaging of anaerobic systems (Mukherjee et al., 2015).

2. AIMS OF THE STUDY

The primary aim of this study is to investigate the intricate relationship between hydrogen peroxide and the transcription factor Nrf2, particularly under physiological oxygen conditions (5 kPa O₂), which more closely resemble *in vivo* environments compared to conventional hyperoxic cell culture conditions. Nrf2 is pivotal in regulating oxidative stress responses, yet the precise role of H₂O₂ in modulating its activity remains a topic of debate. To address this, we developed and employed a novel oxygen-insensitive Nrf2 biosensor, the Pericellular Oxygen-Insensitive Nrf2 Total L^Evel Reporter (POINTER), designed to measure Nrf2 levels independent of oxygen fluctuations. By manipulating intracellular H₂O₂ concentrations through various methods—exogenous H₂O₂ administration, chemogenetic production of H₂O₂ using mDAAO, and pharmacological induction via Auranofin—we aimed to comprehensively assess how different sources and durations of H₂O₂ exposure affect Nrf2 regulation in human cerebral microvascular endothelial cells. Ultimately, this study seeks to shed light on how antioxidant inhibition and H₂O₂ elevation contribute to intracellular Nrf2 levels, particularly under physiological oxygen levels, offering insights into the cellular redox regulation mechanisms.

3. MATERIALS

3.1. Chemicals

Chemicals used during this thesis study are listed in **Appendix A.**

3.2. Equipments

Equipment used during this thesis study is listed in **Appendix B.**

3.3. Molecular Biology Kits

Molecular biology kits used in this thesis study are listed in **Appendix C**.

3.4. Enzymes

All restriction enzymes were provided from New England Biolabs (NEB).

4. METHODS

The methodology used in this study is summarized in Figure 4.1.

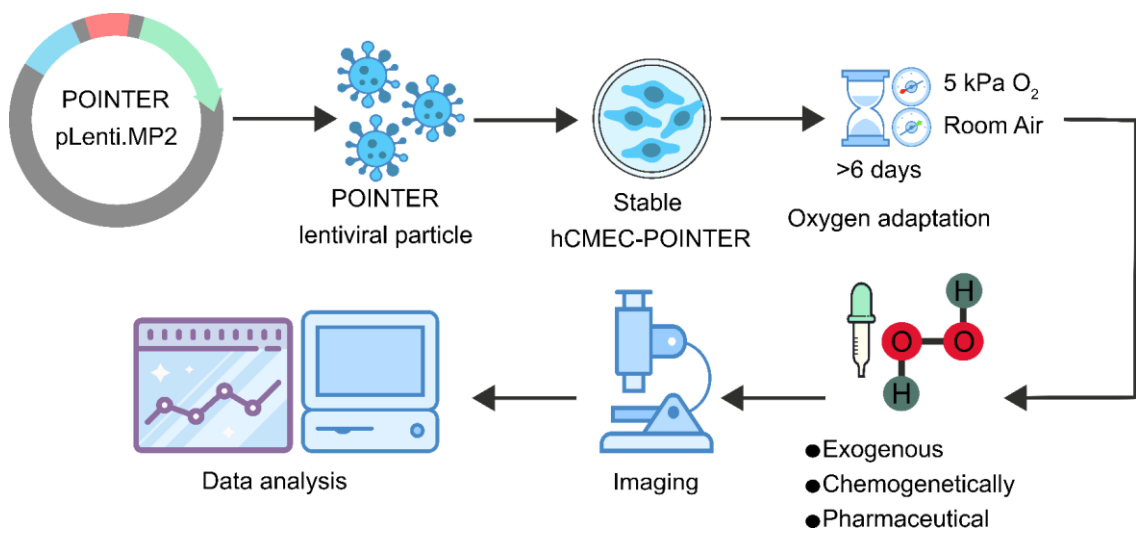


Figure 4.1. Schematic representation of main methodology used in this study.

4.1. Transformation Protocol

Ice-thawed competent DH5 α cells were mixed with 10 pg-1 μ g of plasmid DNA in 50 μ l of the bacterial suspension. After 30 minutes on ice, a 45-second heat shock was applied at 42°C, followed by another 5-minute incubation on ice. The cells were then mixed with 400 μ l LB medium and incubated at 37°C, 220 rpm for one hour. Ampicillin-containing agar plates were pre-warmed at 37°C, and after incubation, the whole cell mixture was spread on the selection plates. The plates were incubated overnight at 37°C. Colonies were picked the following day, and glycerol stocks were prepared for long-term storage at -80°C.

4.2. Cloning

The POINTER vector was constructed by incorporating four consecutive ARE specific to NQO1. These elements were followed by a minimal promoter (minP) and a miniGFP gene that served as the reporter, as detailed in Table 4.1. To assemble the lentiviral plasmid, a codon-optimized miniGFP sequence sourced from Twist Bioscience (San Francisco, CA, USA) was inserted into the EGFP.pTRAF.pLJM1 plasmid, which already housed the ARE and minP sequences. This insertion was carried out using AgeI and EcoRI restriction enzymes. The fully assembled POINTER sequence was then transferred into the EGFP.pTRAF.pLenti.MP2 vector (Addgene #36097) via NheI and XhoI restriction sites. Similarly, existing pLenti.MP2-based plasmids (Addgene #36097), including mCherry.mDAAO and HyPer 7.2, were adapted for targeting either the cytosol or mitochondria, and used to generate the appropriate lentiviral particles.

Table 4.1: The sequence of ARE, minP, miniGFP, and the forward and reverse primers used for the construction of POINTER biosensor.

Sequence Name	Nucleotide Sequence (5' to 3')
Antioxidant Response Element (ARE) for NQO1	TGCAAAATCGCAGTCACAGTGA CT CAGCAGAATCT GAGCCTAGG
minP	TAGAGGGTATATAATGGAAGCTCGACTTCCAG
miniGFP	ATGGAGAAATCCTTCGTCATCACAGACCCcTGGTTG CCAGATTACCCCAATTATTTCTGCCAGTGACGGGTTT TTAGAGCTGACGGAGTACAGCAGAGAGGAAATTAT GGGGCGTAACGCCAGGTTCTTGCAGGGGCCAGAG ACTGACCAGGCAACCGTGCAGAAGATTAGAGACG CTATTAGAGACCGACGGCCCACCACCGTACAGTTG ATCAATTATACAAAGTCAGGCAAGAAATTCTGGAA CCTCTTGCACCTGCAACCCGTGTTTCGACGGTAAAG GCGGACTCCAATACTTCATTGGCGTTCAACTGGTT GGCTCCGATCATGTA
Forward Primer	ATAACCGGTACGCGTGCCACCATGGAGAAATCCTT CGTC
Reverse Primer	ATAGAATTCGTCGACTCTAGAACAATTGTACATGAT CGGAGC

4.3. Plasmid Extraction

A 50 mL (midiprep) or 3-10 mL (miniprep) LB culture was supplemented with the appropriate antibiotic (1:1000 dilution), and a sample of frozen bacteria from glycerol stock was added. The culture was incubated overnight at 37°C with shaking at 220 rpm. The cells were then collected by centrifugation at 4000 rpm for 30 minutes at 4°C. The plasmid was isolated using Qiagen MidiPrep or NEB Monarch Plasmid Miniprep Kits. The concentration and purity were measured using a NanoDrop spectrophotometer, and the plasmid was used for further cloning or transfection experiments.

4.4.Lentivirus production and purification

For small-scale lentivirus production, HEK293T cells with a passage number under 20 were seeded into four 10 cm dishes per viral preparation experiment. The cells were incubated at 37°C until they reached approximately 90% confluency the next day. Before transfection, the medium in each dish was replaced with 10 mL of fresh DMEM (high glucose) one hour prior to transfection. The transfection complex was prepared by using two separate solutions. In one tube, 6 µg of the main plasmid (pLenti-MP2), 3 µg of psPAX2, and 3 µg of pMD.2 were diluted in 500 µL of serum-free DMEM. In another tube, 20 µL of PolyJet transfection reagent was diluted in 500 µL of serum-free DMEM. The PolyJet solution was immediately added to the DNA mixture and incubated for 15 minutes at room temperature, ensuring the incubation time did not exceed 20 minutes. A total of 1000 µL of the transfection complex was then added dropwise to each dish, and the plates were incubated at 37°C.

Twenty-four hours after transfection, the media in each dish was replaced with 10 mL of fresh DMEM. Forty-eight hours post-transfection, the virus-containing media was harvested into 50 mL Falcon tubes (harvest 1), and 10 mL of fresh DMEM was added to each dish. The plates were returned to the incubator for another 24 hours. Seventy-two hours post-transfection, a second harvest (harvest 2) of virus-containing media was collected into 50 mL Falcon tubes. The collected media from both harvests was centrifuged at 300 x g for 5 minutes to remove any remaining cells. The supernatant was passed through a 0.45 µm sterile filter.

For virus purification, the filtered media was processed using the sugar cushion method. A sucrose-containing buffer was prepared by dissolving 20 g of sucrose in 50 mM Tris-HCl (pH 7.4), 100 mM NaCl, and 0.5 mM EDTA. This buffer was sterile-filtered with a 0.22 µm filter. Ten milliliters of the sucrose buffer was added to a 50 mL tube, and 40 mL of the virus-containing media was carefully layered on top of it without mixing the two layers. The tubes were centrifuged at 10,000 x g for 4 hours at 4°C. After centrifugation, the supernatant was carefully removed, first the media layer and then the sucrose buffer, ensuring the viral pellet was not disturbed. The pellet in each falcon was

resuspended in 100 μ L PBS, aliquoted in 20 μ L volumes, and stored at -80°C for long-term use.

4.5. Cell Culture

Human cerebral microvascular endothelial cells, a wild-type line originally purchased from CELLutions BIOSYSTEMS (CLU512), were generously provided by the laboratories of Richard Siow and Giovanni Mann (King's College London, UK). The cells were cultured in endothelial cell growth medium (CURIO BIOTECH, CB-EC-GM, VS, Switzerland), supplemented with 50 U/mL penicillin-streptomycin (Gibco, 25200056, MA, USA), 1X antibiotic-antimycotic (Gibco, 15140122, MA, USA), and 1X Normocin (Invivogen, ant-nr-1, CA, USA). All experiments were conducted using hCMEC/D3 cells between passages 28 and 38. The cells were maintained under standard cell culture conditions of 37°C and 5% CO_2 , either in room air (hyperoxia) or in normoxic conditions (5 kPa O_2).

For viral transduction, hCMEC/D3 cells were plated in 6-well plates using antibiotic-free medium, supplemented with 10 $\mu\text{g}/\text{mL}$ Polybrene (Sigma-Aldrich, St. Louis, MO, USA) and the appropriate lentiviral particles. Following transduction, cells were cultured in virus-containing medium for 48–72 hours. After this period, the medium was replaced with complete endothelial growth medium, and cells were cultured for one week before being subjected to fluorescence-activated cell sorting (FACS). Sorting was performed using a B.D. Influx Cell Sorter, with 488 nm and 561 nm lasers for green (POINTER, HyPer7.2) and red (mCherry.mDAAO) fluorescence, respectively. The gating strategy involved isolating positive populations for green, red, or both fluorescence channels. The sorted cell populations were expanded and used in subsequent experiments.

To ensure robust stabilization of HIF-1 α , a key marker of cellular adaptation to oxygen levels (Warpsinski et al., 2020), the cells were maintained in either room air or normoxia

(5 kPa O₂) for a minimum of 5 days prior to any treatment or experimental procedure. Media and solutions were preconditioned to match the respective oxygen levels for at least one day before subculturing the cells.

For experimental assays, cells were seeded onto 6-well plates containing 30 mm coverslips (Glaswarenfabrik Karl Knecht Sondheim, Sondheim vor der Rhön, Germany) the day prior to treatment. For long-term treatment, 24 hours before imaging or analysis, the medium was replaced with fresh hCMEC/D3 medium containing the respective doses of H₂O₂, D-alanine, or Auranofin. The next day, the cells were imaged directly in the same medium.

4.6. Imaging Buffer Preparation

During live-cell imaging, a physiological buffer known as 2CaNa was used to perfuse the cells. The 2CaNa buffer was made with 10 mM HEPES, 2 mM CaCl₂, 138 mM NaCl, 1 mM MgCl₂, 10 mM D-glucose, and 5 mM KCl, with the pH adjusted to 7.42 using 1M NaOH. All other solutions for the imaging experiments, such as amino acids and H₂O₂, were also prepared in this buffer.

4.7. Live-cell Imaging

For live-cell fluorescence imaging, an Axio Observer Z1.7 widefield epifluorescence microscope (Carl Zeiss AG, Oberkochen, Germany) equipped with a Colibri 7 LED light

source, Plan-Apochromat 20×/0.8 dry objective, Plan-Apochromat 40×/1.4 oil immersion objective, and a monochrome CCD camera (AxioCam 503) was employed. Cells were perfused with substrates using a custom peristaltic pump in a metal perfusion chamber (NGFI, Graz, Austria). For HyPer7.2 imaging, alternating LED excitation at 423/44 nm and 469/38 nm was applied using FT455 (HyPer low) and FT495 (HyPer high) beamsplitters. Emissions were detected using a 525/50 nm bandpass filter. POINTER fluorescence was measured using an FT495 excitation filter and a 525/50 nm bandpass emission filter. For mCherry.mDAAO imaging, FT570 (BS) and 605/70 nm filters were used. Both single and dual imaging of HyPer7.2/POINTER and mCherry were performed using this setup. Data acquisition and control were managed through Zen Blue 3.1 Pro software (Carl Zeiss AG, Oberkochen, Germany). A pump-driven, custom-made perfusion system was used for buffer and treatment solutions delivery. This setup featured multiple syringe tubes with manual on-off switches for precise control of stimulations. Solutions were delivered to the cells through plastic capillary tubing connected to the inlet of a metal perfusion chamber. A peristaltic pump ensured a consistent flow rate for buffer and stimulant delivery, while a central vacuum system at the outlet maintained a steady flow, collecting outflow in a disposal flask. The custom-built perfusion system consisted of multiple reservoirs to hold different stimulants, a peristaltic pump to ensure controlled and steady flow to the cells, and a perfusion chamber designed to securely hold 30 mm glass coverslips with live cells. The setup also included a flask for waste collection.

4.8. Confocal Imaging

Confocal microscopy was conducted using a Zeiss LSM 880 laser scanning microscope, equipped with Plan-Apochromat 20×/0.8 and Plan-Apochromat 40×/1.3 oil immersion objectives, to visualize hCMEC/D3 cells expressing POINTER and either mitochondrial or cytosolic HyPer7.2 or mCherry.mDAAO. The Airyscan fast mode was used, with 458

nm and 594 nm lasers for POINTER and mCherry detection, respectively. HyPer Low, HyPer High, and mCherry were excited using 405 nm, 488 nm, and 594 nm lasers, and their emissions were captured with BP 495–550 nm and LP 570 nm filters. Image acquisition was controlled via Zen Black software (Carl Zeiss AG).

4.9.FACS Analysis

To generate dose-response curves for HyPer7.2 in hCMEC/D3 cells exposed to either exogenously applied or chemogenetically produced H₂O₂, and to determine the EC50 values for H₂O₂ and D-alanine, flow cytometric-based analysis was performed using the BD FACSymphony A1 Cell Analyzer (BD Biosciences). Approximately 5×10^5 cells were treated with either H₂O₂ (for 5 minutes) or D-alanine (for 20 minutes) at varying concentrations in PBS. HyPer7.2 fluorescence was captured using a 405 nm laser and a 525/40 nm bandpass filter for the HyPer low signal, and a 480 nm laser with a 530/30 nm bandpass filter for the HyPer high signal. Live cells were gated based on forward scatter (FSC) and side scatter (SSC) properties, excluding debris. The HyPer7.2 ratio was calculated for each cell using FlowJo 10.10.0 software (BD), dividing the HyPer high (Excitation 477 nm, Emission 525 nm) by the HyPer low (Excitation 420 nm, Emission 525 nm) signals. The mean intensity for each well was then used to construct dose-response curves.

4.10. Cell Viability Assay

Propidium iodide (PI) staining was used to assess cell membrane integrity as a measure of viability in hCMEC/D3 cells treated with varying concentrations of H₂O₂, D-alanine, or Auranofin. Cells (three wells per treatment and control group) were incubated with the treatments for 24 hours. After treatment, the cells were harvested, centrifuged at 300 × g for 5 minutes, and resuspended in PBS. Before FACS analysis, PI (1 μL from a 1 mg/mL stock) was added to 1 mL of cell suspension, and samples were incubated for 5 minutes at room temperature. Red fluorescence due to PI staining was detected using a 561 nm laser and a 586/15 nm bandpass filter on the BD FACSymphony A1 analyzer. A total of 10,000 events were collected, and the ratio of PI-positive to total gated cells was calculated to determine the percentage of viable cells.

4.11. Quantitative (Real-Time) PCR

Quantitative PCR was performed to analyze gene expression levels of NRF2, HMOX1, and PRDX1 (using primers listed in table 4.2) in hCMEC/D3 cells cultured under 5 kPa O₂ or room air. Total RNA was extracted using the FastPure Cell/Tissue Total RNA Isolation Kit V2 (Vesyme, RC112-00), and cDNA was synthesized with the HiScript III RT SuperMix for qPCR (+gDNA wiper) kit (Vesyme, R323-01). Quantification of gene expression was carried out using a BIO-RAD CFX Connect Real-Time System and CFX Maestro Software, utilizing Taq Pro Universal SYBR qPCR Master Mix (Vesyme, Q712-02). Data were normalized to β-actin expression, and the 2- $\Delta\Delta$ CP method was used for relative quantification.

Table 4.2: List of primers used for real time qPCR.

Primer Name	Species	Cat#	Primer DNA sequence
β -actin forward primer	Human	HP204660	CACCATGGCAATGAGCGGTTC
β -actin reverse primer	Human	HP204660	AGGTCTTTGCGGATGTCCACGT
NRF2 (NFE2L2) forward primer	Human	HP209154	CACATCCAGTCAGAAACCAGTGG
NRF2 (NFE2L2) reverse primer	Human	HP209154	GGAATGTCTGCGCCAAAAGCTG
Heme oxygenase 1 (HMOX1) forward primer	Human	HP205872	CCAGGCAGAGAATGCTGAGTTC
Heme oxygenase 1 (HMOX1) reverse primer	Human	HP205872	AAGACTGGGCTCTCCTTGTTGC
Peroxiredoxin 1 (PRDX1) forward primer	Human	HP206233	CTGCCAAGTGATTGGTGCTTCTG
Peroxiredoxin 1 (PRDX1) reverse primer	Human	HP206233	AATGGTGCGCTTCGGGTCTGAT

4.12. Data Analysis

The HyPer7.2 biosensor, characterized by two excitation wavelengths and a single emission, was analyzed by calculating the ratio of HyPer high (Ex = 480 nm) to HyPer low (Ex = 430 nm). For time-lapse imaging, HyPer ratios were normalized to baseline values. To assess HyPer7.2 or POINTER signals after 24 hours of treatment, four snapshots were taken from each well, and the mean intensity of five cells per image was measured. Background subtraction was applied using Microsoft Excel, and the normalized data were used to compute the HyPer ratios or POINTER signals.

4.13. Statistical Analysis

All statistical analyses were conducted using GraphPad Prism Software version 10.2.3. Experiments were performed in triplicate, and data are presented as means \pm SD or SEM. Statistical significance was calculated using one-way ANOVA with Tukey's post-hoc test for multiple comparisons or Student's t-test for pairwise comparisons. P-values greater than 0.05 were considered non-significant.

5. RESULTS

5.1. Principle and Validation of the Oxygen-Independent Biosensor: POINTER

The development of a novel, oxygen-independent biosensor for studying Nrf2 regulation under varying oxygen conditions is depicted in Figure 5.1.A. The biosensor, named POINTER (Pericellular Oxygen Insensitive Nrf2 Total Level Reporter), was created by adapting the pTRAF system developed by Johansson et al. (Johansson et al., 2017), and engineered into a miniGFP-based Nrf2 reporter. The innovative feature of this sensor lies in its ability to function independently of oxygen availability, addressing a crucial gap in studying cellular redox states, particularly in hypoxic environments. POINTER was designed to quantify total cellular Nrf2 levels, providing a real-time readout of Nrf2 activity irrespective of fluctuations in oxygen levels.

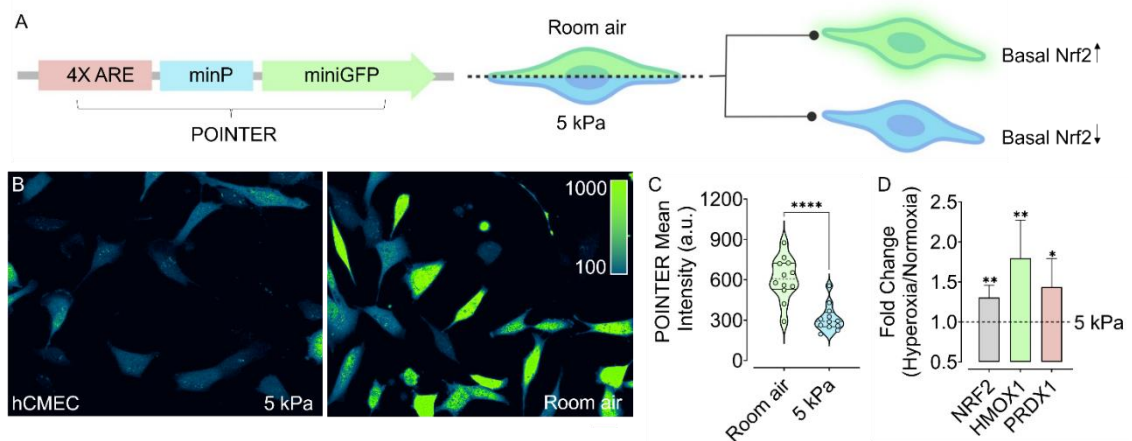


Figure 5.1. Functionality and Application of the POINTER Biosensor. (A) Diagram of the POINTER biosensor, designed to report intracellular Nrf2 levels in both hyperoxic (room air) and normoxic (5 kPa O₂) environments. (B) Confocal microscopy of hCMEC/D3 cells expressing POINTER, adapted for over 5 days to room air (right) or 5 kPa O₂ (left). Scale bar: 50 μm. (C) Violin plots displaying POINTER fluorescence in hCMEC/D3 cells adapted to 5 kPa (blue, n=3/60) and room air (green, n=3/60) conditions. (D) Fold changes in the transcription of redox-regulating genes, with the dashed line marking baseline expression at 5 kPa O₂. Data are Mean ± SD from four biological replicates. Unpaired t-tests were conducted to compare 5 kPa to room air in panels C and D. (Figure taken from (Miri et al., 2024))

One key motivation for developing POINTER was the limited applicability of existing Nrf2 reporters in low-oxygen or hypoxic environments. Traditional reporters are dependent on oxygen-sensitive processes that can obscure the precise measurement of Nrf2 under such conditions. POINTER was designed to overcome these limitations, thus enabling a more accurate and reliable assessment of Nrf2 dynamics across a range of oxygen concentrations. To validate the biosensor's functionality, we utilized human brain endothelial cells as a model system. These cells were chosen because they are well-established in studies of vascular biology, particularly in the context of the blood-brain barrier and oxidative stress responses, and they represent a relevant cellular context for examining Nrf2 regulation in response to oxidative stress.

Due to the inherent difficulty in transiently transfecting hCMEC/D3 cells—an obstacle often encountered when working with primary endothelial cells—we employed lentiviral vectors to ensure stable expression of the POINTER construct (Figure 5.1.B). Lentiviral vectors provide an efficient means of achieving long-term expression, allowing us to bypass the challenges of transient transfection and ensuring consistent expression levels of the reporter. The stable expression of POINTER, HyPer7.2, and mCherry.mDAAO in these cells was confirmed through FACS, which demonstrated a homogeneous population of cells expressing the biosensor (Figure 5.2). This stable integration (Figure 5.3) enabled us to conduct long-term experiments, eliminating variability in expression that could confound the results.

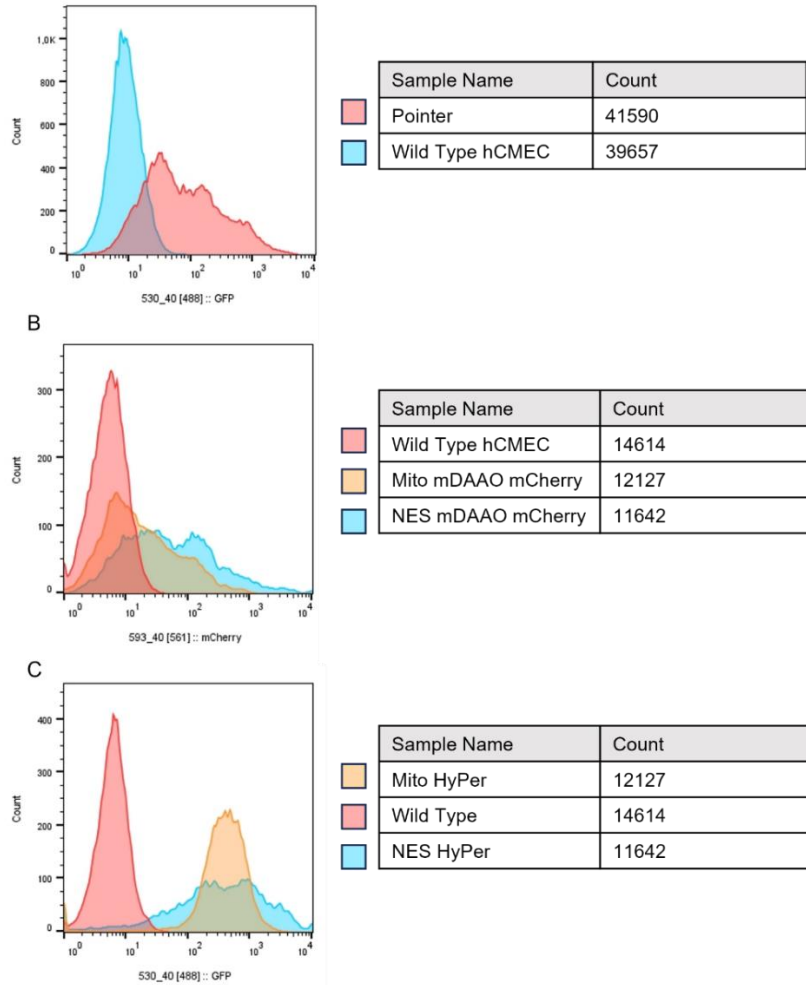


figure 5.2. FACS diagrams of hCMEC/D3 cells. The FACS diagrams of hCMEC/D3 cells expressing A) POINTER, B) mCherry.mDAAO, and C) HyPer7.2. (Figure taken from (Miri *et al.*, 2024))

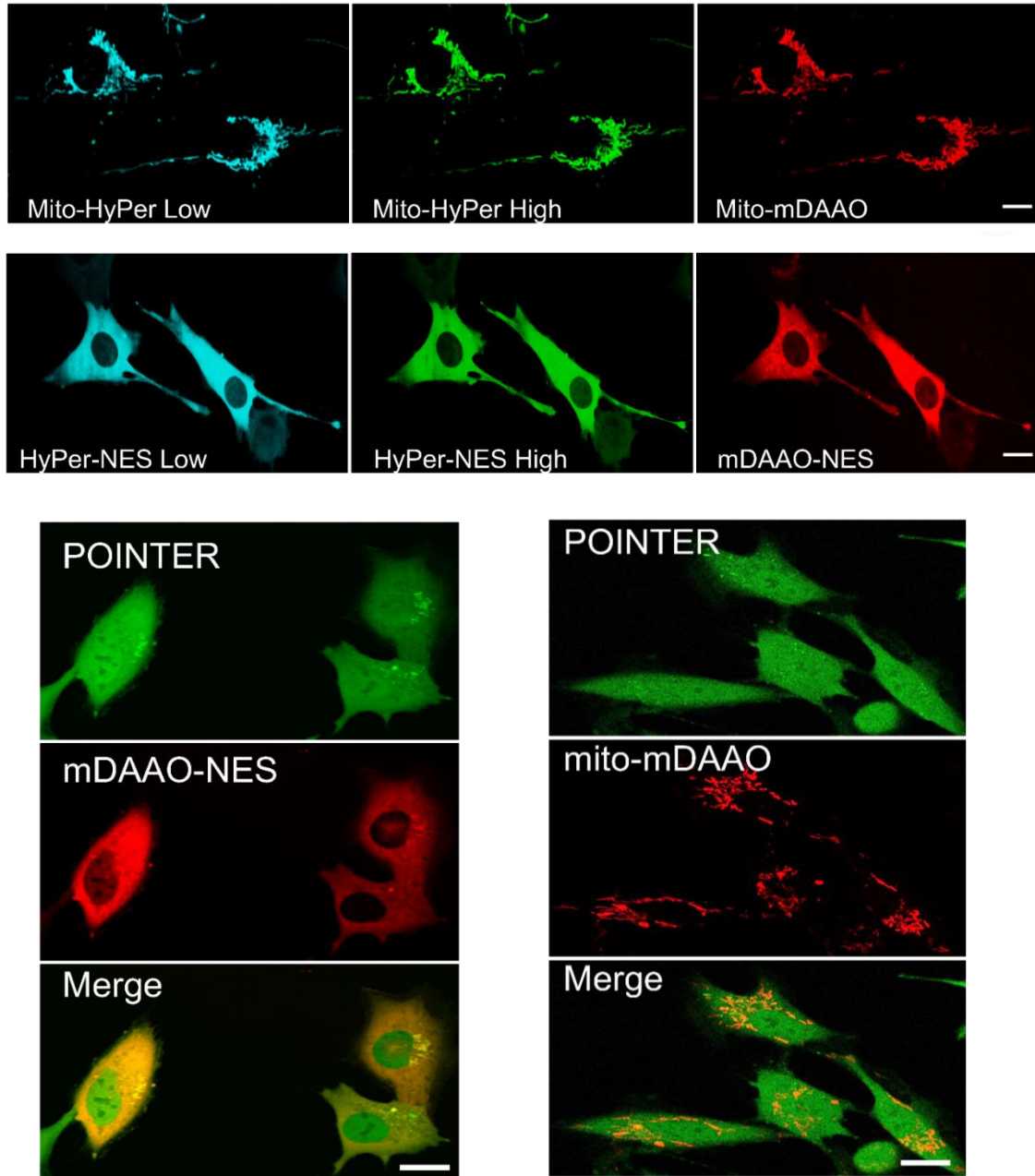


Figure 5.3. Representative confocal images of hCMEC/D3 cells expressing HyPer7.2 and mCherry.mDAAO in the mitochondria (top row) or the cytosol (bottom row)

5.2. Assessing POINTER's Functionality in Different Oxygen Conditions

To test the functionality of the POINTER biosensor, we aimed to replicate the findings of previous studies that indicated higher Nrf2 levels in cells cultured under high pericellular oxygen (room air) compared to those cultured under physiological normoxia

(5 kPa). Notably, (Chapple et al., 2016) and (Warpsinski *et al.*, 2020) demonstrated that Nrf2 levels are elevated in cells exposed to ambient oxygen (21% O₂, commonly referred to as room air) but are significantly lower when cells are adapted to more physiological oxygen levels. To investigate this phenomenon, we cultured hCMEC/D3 cells under both room air and 5 kPa O₂, hypothesizing that Nrf2 levels would be elevated under room air conditions, consistent with previous findings.

Figures 5.1.B and 5.1.C confirm our hypothesis: cells adapted to room air showed significantly higher POINTER signals compared to those cultured under 5 kPa normoxia. The difference in POINTER signals between the two oxygen conditions directly correlates with the known upregulation of Nrf2 in response to oxidative stress in hyperoxic environments. These results validate the functionality of POINTER as an accurate reporter of Nrf2 levels under varying oxygen conditions, demonstrating that the sensor is capable of detecting fluctuations in Nrf2 levels that occur in response to differences in pericellular oxygen.

The functionality of POINTER was further corroborated by real-time PCR analysis of key oxidative stress-related transcripts (Figure 5.1.D). Cells cultured in room air exhibited significantly higher levels of oxidative stress markers compared to those adapted to 5 kPa, mirroring the changes in Nrf2 levels detected by the POINTER biosensor. This finding supports the notion that elevated Nrf2 levels in room air correspond to increased oxidative stress, while physiological normoxia results in a reduction in both oxidative stress and Nrf2 activity. These results collectively validate POINTER as an effective tool for studying Nrf2 regulation across different oxygen environments, providing new insights into the oxygen-dependent dynamics of Nrf2 signaling.

5.3. Investigating the Relationship Between Oxidative Stress and Nrf2 Using Three Approaches to Manipulate H₂O₂ Levels

After confirming the functionality of POINTER, we aimed to explore the relationship between cellular oxidative stress—particularly H_2O_2 —and Nrf2 levels. To manipulate intracellular H_2O_2 levels, we employed three distinct approaches: exogenous application of H_2O_2 , chemogenetic-based production using DAAO, and pharmacological induction via Auranofin.

5.3.1. Exogenous Application of H_2O_2

In this approach, we directly applied varying concentrations of H_2O_2 (1–50 μM) to hCMEC/D3 cells and monitored the response using the HyPer7.2 biosensor, which specifically detects H_2O_2 . The HyPer7.2 ratio, which reflects changes in H_2O_2 levels, was measured in both the cytosol (Figure 5.4.A) and mitochondria (Figure 5.4.B). We observed a detectable increase in the HyPer7.2 ratio at 1 μM H_2O_2 , with the biosensor reaching saturation at approximately 30 μM . This rapid, dose-dependent response indicates that hCMEC/D3 cells efficiently take up exogenously applied H_2O_2 , with the HyPer7.2 ratio stabilizing within minutes after each dose (Figure 5.5).

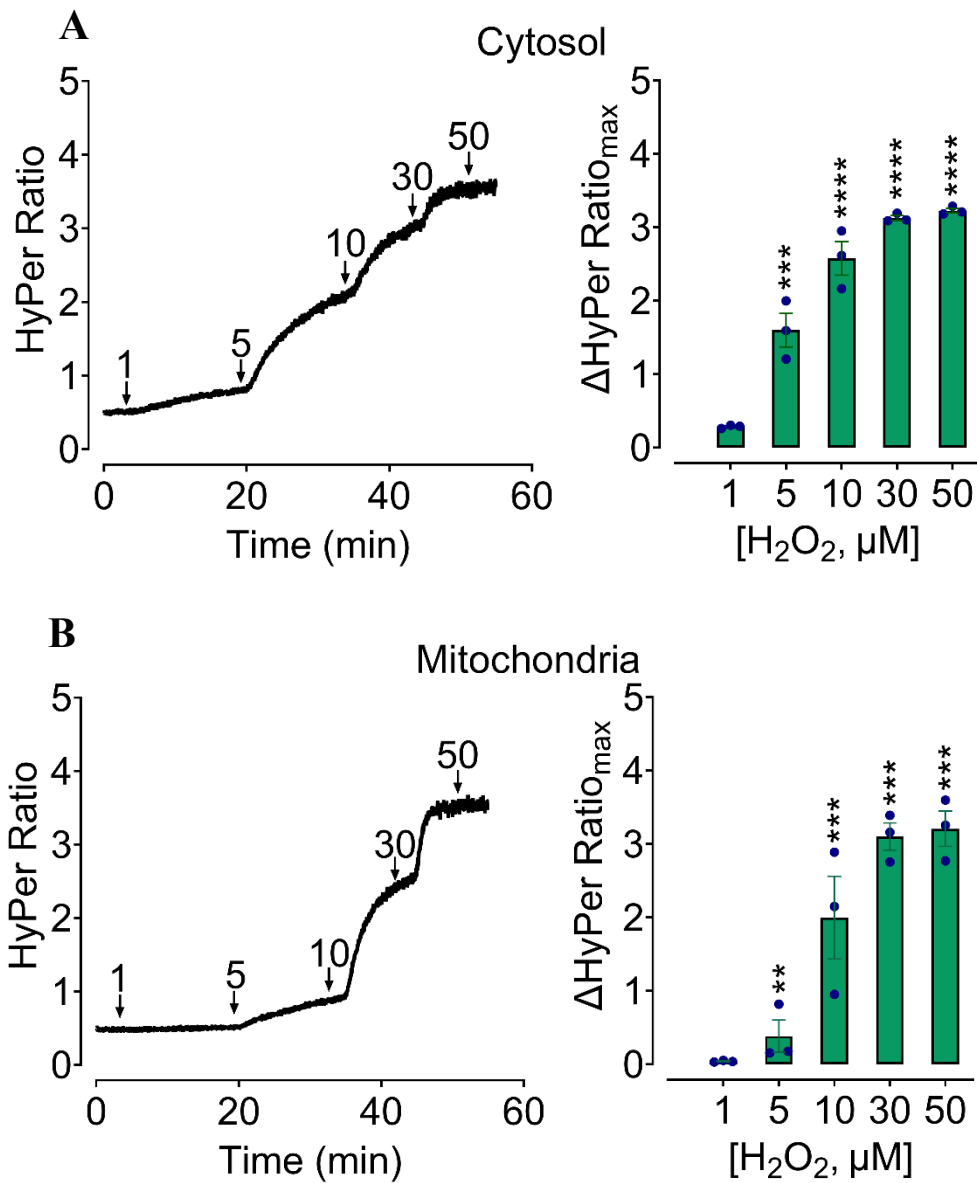


Figure 5.4. HyPer7.2 Biosensor Response to H₂O₂ in Cytosol and Mitochondria. (A) The HyPer7.2 ratio, representing cytosolic H₂O₂ levels, was measured in hCMEC/D3 cells at varying concentrations of exogenously applied H₂O₂. (B) A similar dose-dependent response was observed in the mitochondria, with rapid stabilization of the HyPer7.2 ratio after each dose. Bar graphs in both panels compare the maximum HyPer7.2 response at each concentration to basal levels, with significant differences between each concentration and lowest dose determined by t-test (**P≤0.01, ***P≤0.001, ****P≤0.0001).

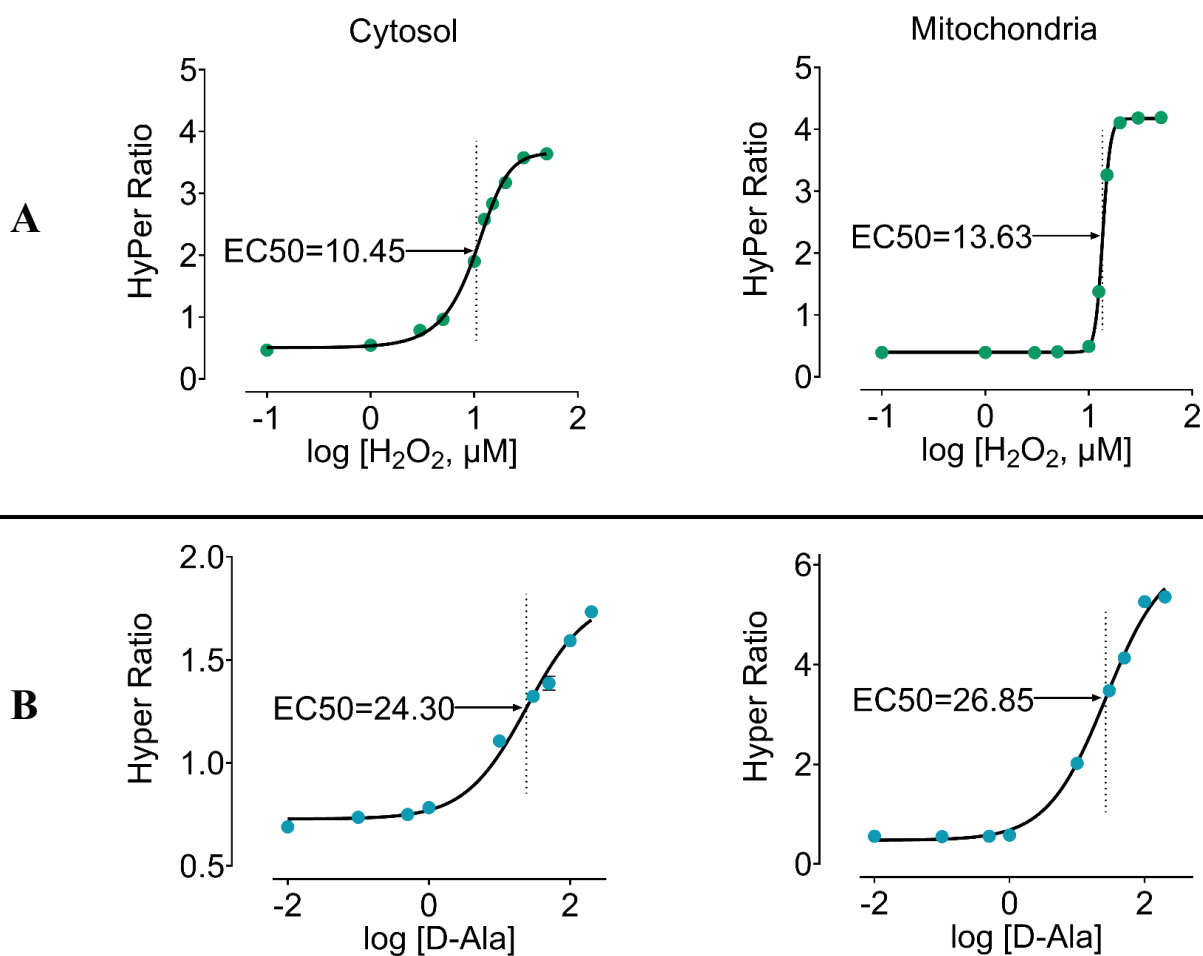


Figure 5.5. Dose-response curves of hCMEC/D3 expressing cytosolic (left) or mitochondrial (right) HyPer7.2 and mCherry.mDAAO in response to H₂O₂ (A) or D-alanine (B). All data points represent the mean±SEM of three biological replicates (N=3).

However, while this method provides a robust means of elevating intracellular H₂O₂, it does not allow for precise control over the subcellular localization of H₂O₂, as the entire cell is uniformly exposed to the applied H₂O₂.

5.3.2. Chemogenetic Production of H₂O₂

To achieve greater spatiotemporal control over H₂O₂ production, we employed a chemogenetic approach using DAAO, which catalyzes the oxidation of some D-amino acids like D-alanine to produce H₂O₂. We generated mDAAO constructs to target either the cytosol or mitochondria of hCMEC/D3 cells, allowing for compartment-specific H₂O₂ generation upon the addition of D-alanine. When D-alanine was added at concentrations of 1, 10, and 30 mM, we observed a delayed but dose-dependent increase in the HyPer7.2 ratio in both the cytosol (Figure 5.6.A) and mitochondria (Figure 5.6.B). This delay likely reflects the time required for D-alanine to diffuse into the cells and for mDAAO to catalyze H₂O₂ production (Figure 5.5). Following the addition of 50 μM exogenous H₂O₂, a substantial increase in the HyPer7.2 ratio was observed, indicating that the system is responsive to both endogenous and exogenous sources of H₂O₂.

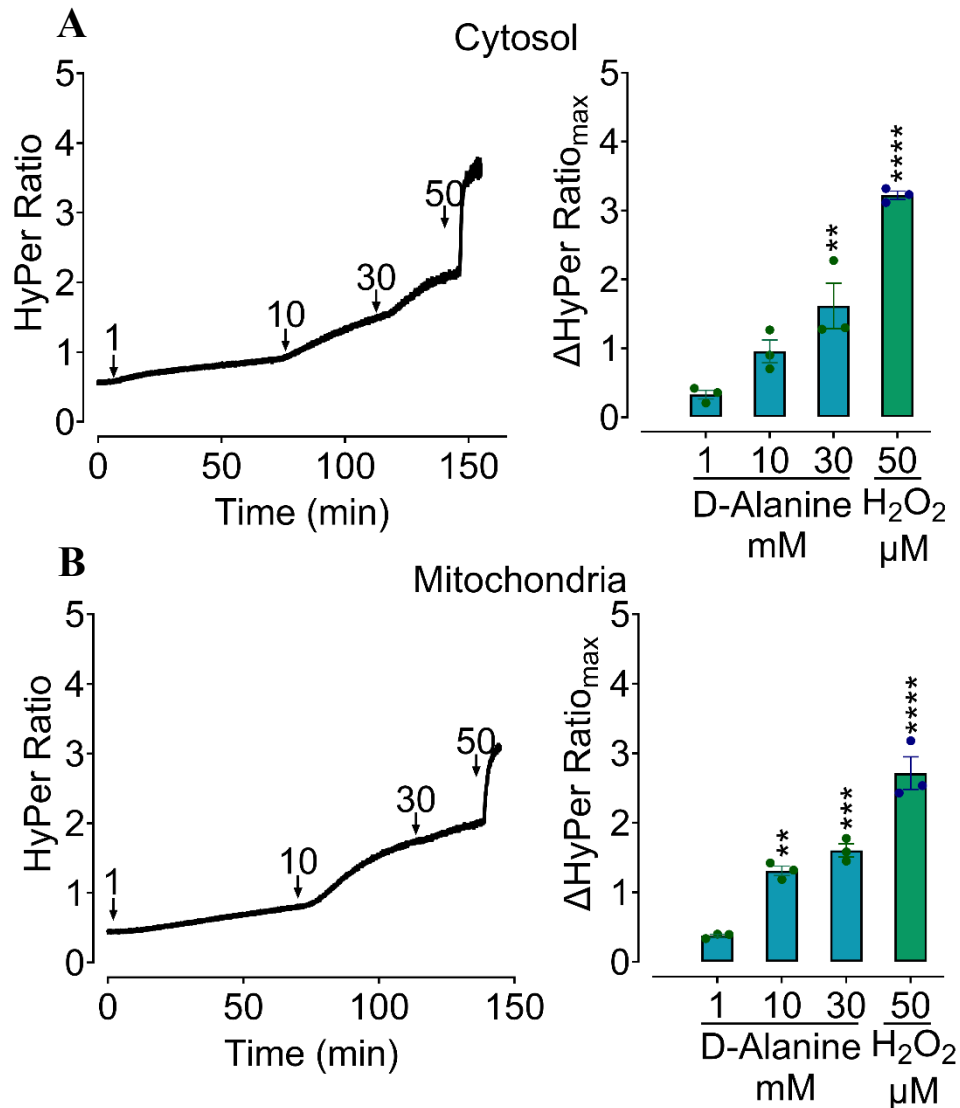


Figure 5.6. Chemogenetic Control of H₂O₂ Production Using DAAO in Cytosol and Mitochondria. (A) The cytosolic HyPer7.2 ratio was measured in hCMEC/D3 cells expressing mDAAO after the addition of D-alanine at concentrations of 1, 10, and 30 mM followed by administration of 50 μM from H₂O₂. (B) A similar response was recorded in mitochondria-targeted mDAAO constructs. Bar graphs in both panels compare the maximum HyPer7.2 response at each concentration to basal levels, with significant differences between each concentration and lowest dose determined by t-test (**P≤0.01, ***P≤0.001, ****P≤0.0001).

5.3.3. Pharmacological Induction of H₂O₂

The third approach involved the pharmacological agent Auranofin, which inhibits thioredoxin reductase, a key component of the cellular antioxidant machinery. By disrupting the antioxidant defenses of the cell, Auranofin indirectly increases

intracellular H_2O_2 levels. We treated hCMEC/D3 cells with a sublethal dose ($0.2 \mu\text{M}$) (Figure 5.7) of Auranofin and measured the resulting changes in H_2O_2 levels using the HyPer7.2 biosensor. In both the cytosol (Figure 5.8.A) and mitochondria (Figure 5.8.B), we observed a gradual increase in the HyPer7.2 ratio, with levels plateauing after approximately 50 minutes. The maximum H_2O_2 levels achieved through Auranofin treatment were comparable to those observed with $5 \mu\text{M}$ exogenous H_2O_2 or 30 mM D-alanine, indicating that this approach effectively elevates intracellular H_2O_2 .

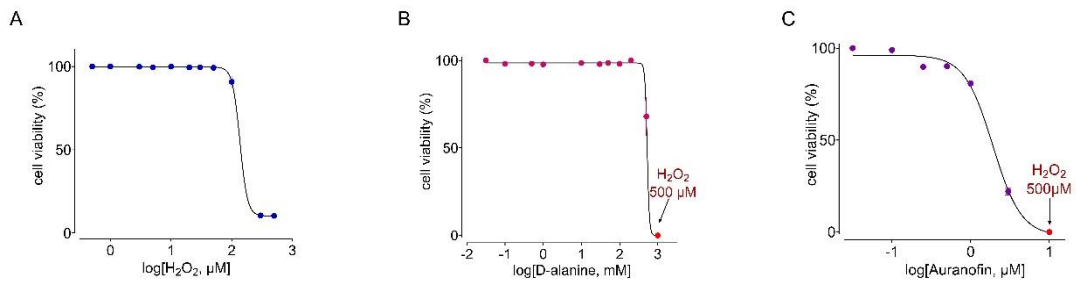


Figure 5.7. The cell viability results of (A) H_2O_2 , (B) D-alanine, and (C) Auranofin. (Figure taken from (Miri *et al.*, 2024))

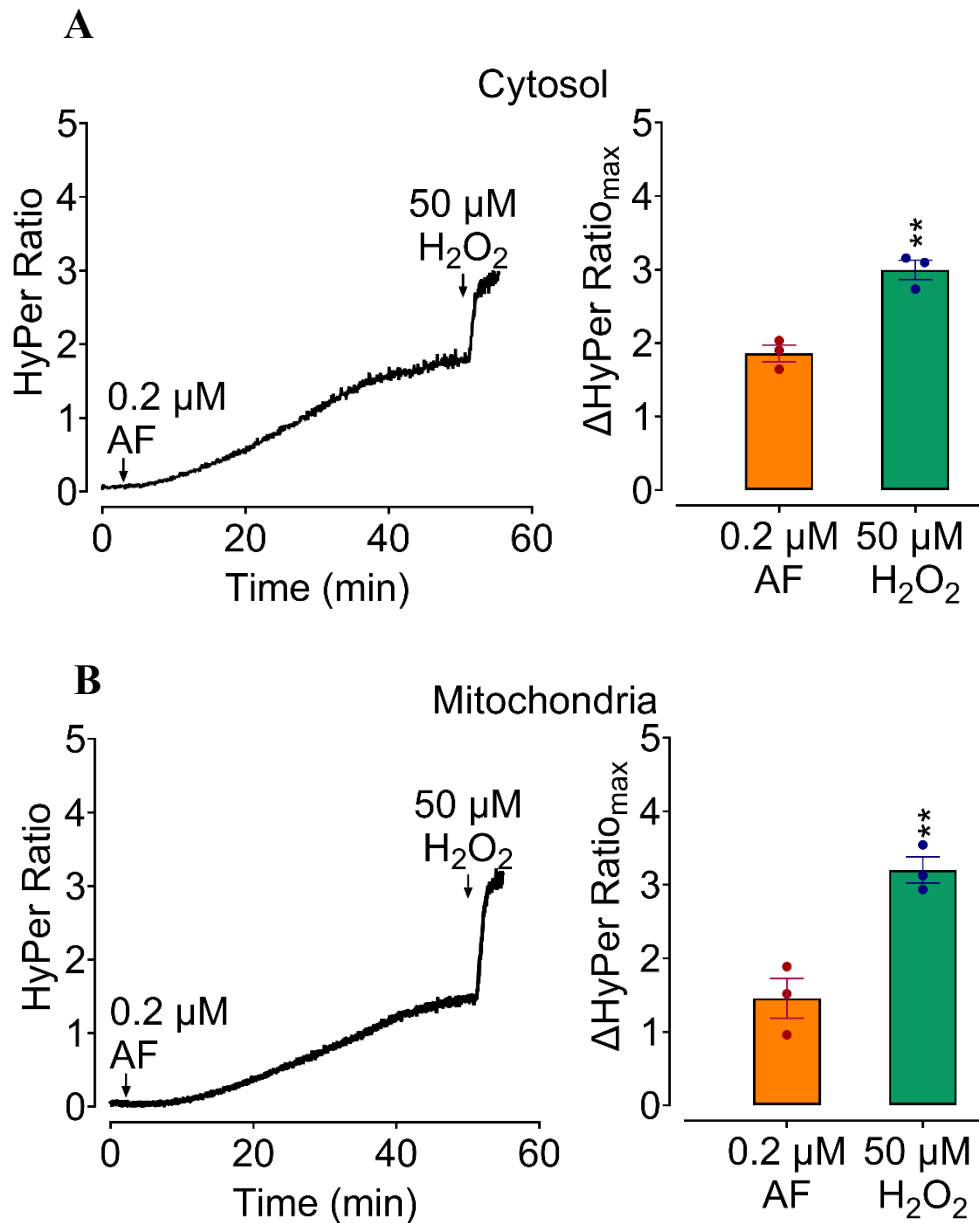


Figure 5.8. Auranofin-Induced Elevation of Intracellular H₂O₂ in hCMEC/D3 Cells. The effects of Auranofin treatment (0.2 μM) on H₂O₂ levels in the cytosol (A) and mitochondria (B), respectively, as measured by the HyPer7.2 biosensor. Bar graphs in both panels compare the maximum HyPer7.2 response at each condition to basal levels, with significant differences between Auranofin and 50 μM exogenous H₂O₂

5.4. Persistent Versus Transient H₂O₂ Responses and Their Impact on Nrf2 Activation

Having established that each of the three approaches effectively elevates intracellular H_2O_2 , we next sought to determine how long these elevated H_2O_2 levels persist and their subsequent effects on Nrf2 activation. To this end, we measured intracellular H_2O_2 levels 24 hours after treatment with H_2O_2 , D-alanine, or Auranofin. Additionally, we accounted for pericellular oxygen levels, as cells were adapted to either room air or 5 kPa O_2 for at least five days prior to treatment to allow for full adaptation of oxygen-sensing pathways, including the normalization of hypoxia-inducible factor 1-alpha (HIF1- α).

In the case of exogenous H_2O_2 treatment (Figure 5.9), no detectable H_2O_2 remained in either the cytosol (Figure 5.9.A) or mitochondria (Figure 5.9.B) 24 hours after treatment, regardless of the initial dose. These results suggest that hCMEC/D3 cells efficiently clear bolus administered H_2O_2 within 24 hours, likely due to their robust antioxidant defenses. Importantly, this clearance occurred under both room air and 5 kPa conditions, indicating that the cells' ability to detoxify H_2O_2 is not significantly altered by oxygen availability.

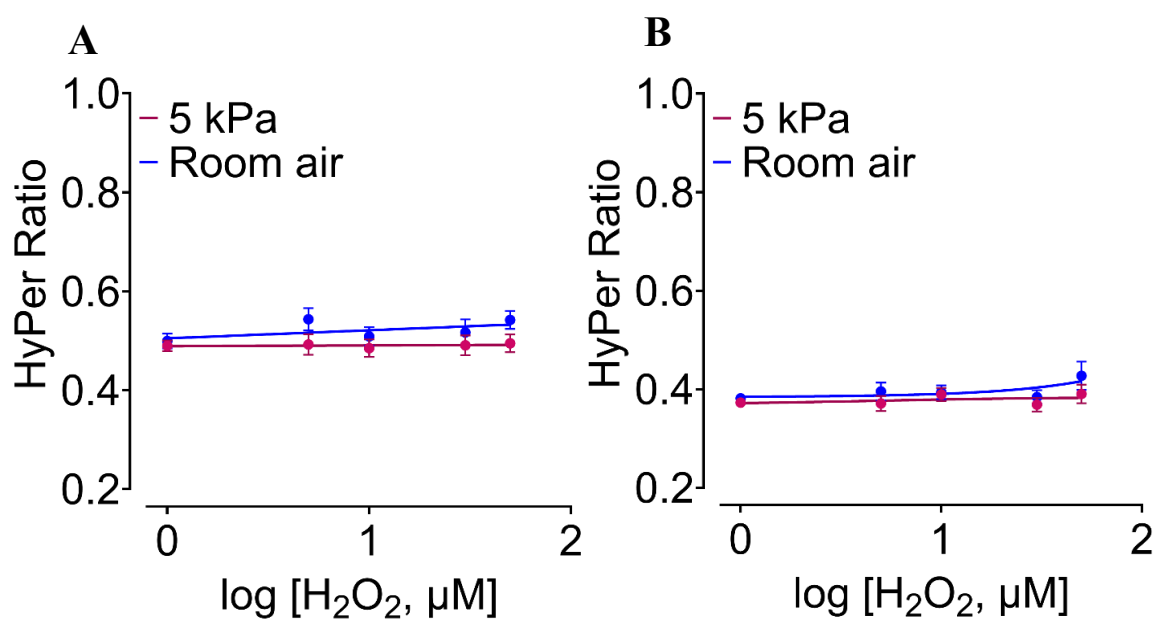


Figure 5.9. Clearance of Exogenously Administered H_2O_2 in hCMEC/D3 Cells After 24 Hours. (A) HyPer7.2 responses of hCMEC/D3 cells treated with exogenous H_2O_2 . After 24 hours. No detectable H_2O_2 remains in the cytosol, regardless of the initial H_2O_2 concentration or oxygen conditions (room air vs. 5 kPa). (B) Mitochondrial HyPer7.2 responses showing similar results, with no residual H_2O_2 detected 24 hours post-treatment. All data points represent the mean \pm SEM of three

biological replicates (N=3), each showing the mean of 12 snaps (n=12) and 5 cells were picked for analysis in each frame (n'=60).

In contrast, cells treated with D-alanine to induce chemogenetic production of H₂O₂ via mDAAO exhibited sustained H₂O₂ levels 24 hours after treatment (Figure 5.10). The persistence of H₂O₂ was dose-dependent, with higher concentrations of D-alanine leading to greater H₂O₂ retention in both the cytosol (Figure 5.10.A) and mitochondria (Figure 5.10.B). Interestingly, cells cultured under physiological normoxia (5 kPa) showed a greater retention of H₂O₂ compared to those cultured in room air, suggesting that lower oxygen levels enhance the cells' capacity to maintain oxidative stress over prolonged periods.

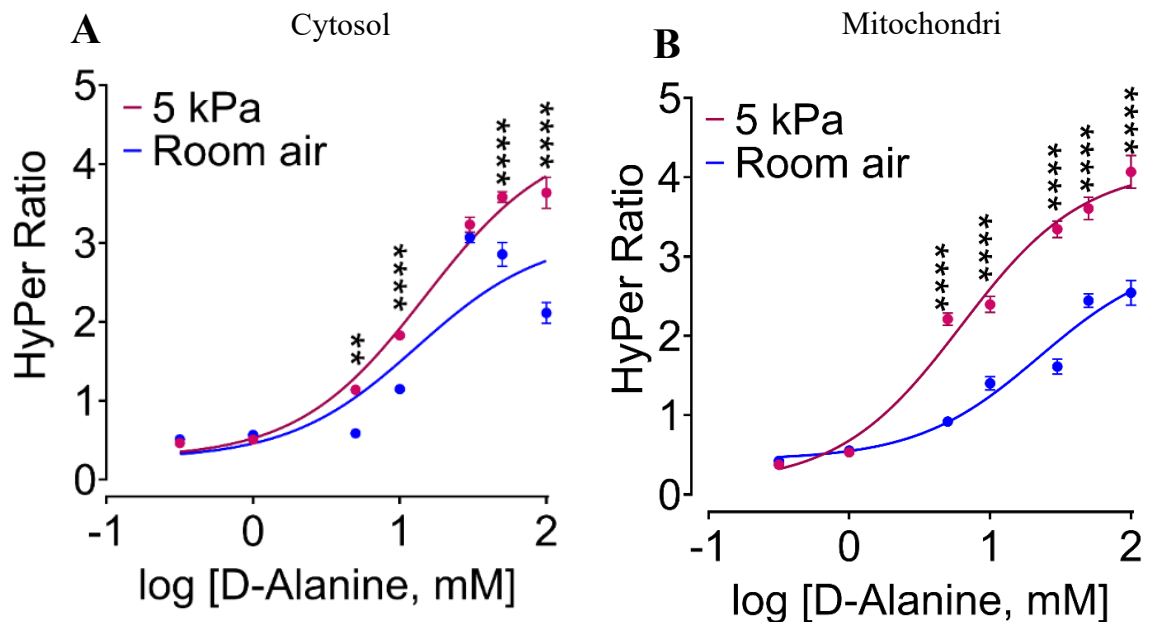


Figure 5.10. Sustained H₂O₂ Levels in hCMEC/D3 Cells After Chemogenetic H₂O₂ Production. (A) Cytosolic HyPer7.2 ratio in hCMEC/D3 cells 24 hours after D-alanine-induced H₂O₂ production through mDAAO. Higher concentrations of D-alanine led to increased and sustained H₂O₂ levels in the cytosol. (B) Mitochondrial HyPer7.2 ratio showing similar dose-dependent retention of H₂O₂ in the mitochondria. Cells cultured under physiological normoxia (5 kPa) exhibited greater H₂O₂ retention compared to cells in room air. All data points represent the mean±SEM of three biological replicates (N=3), each showing the mean of 12 snaps (n=12) and 5 cells were picked for analysis in each frame (n'=60). All statistical analysis were performed using one-way ANOVA with Tukey's multiple comparison post-test. **P≤0.01, ***P≤0.001.

Finally, Auranofin treatment (Figure 5.11) resulted in relatively low levels of H₂O₂ remaining 24 hours after treatment, particularly in the cytosol. However, a clear difference was observed between cells cultured in room air and those adapted to 5 kPa: cells in the 5 kPa group exhibited significantly lower H₂O₂ levels, likely due to enhanced antioxidant capacity under physiological oxygen conditions.

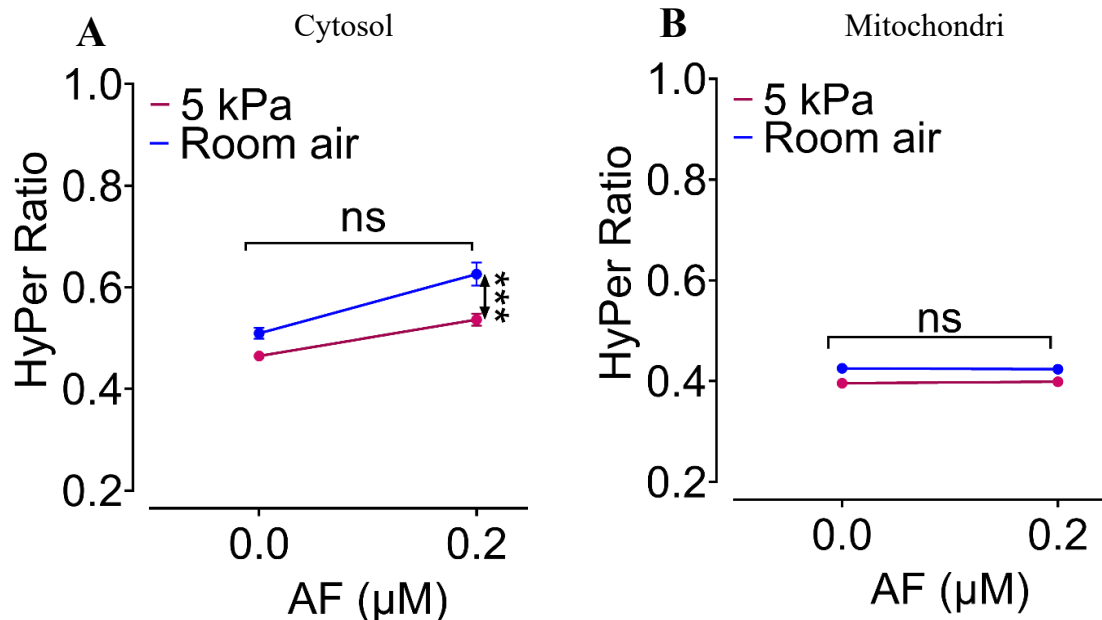


Figure 5.11. Residual H₂O₂ Levels in hCMEC/D3 Cells 24 Hours After Auranofin Treatment. HyPer7.2 responses Following Auranofin treatment in the cytosol (A) and mitochondria (B) of hCMEC/D3 cells adapted to whether room air or 5 kPa O₂. All data points represent the mean±SEM of three biological replicates (N=3), each showing the mean of 12 snaps (n=12) and 5 cells were picked for analysis in each frame (n'=60). All statistical analysis were performed using one-way ANOVA with Tukey's multiple comparison post-test. ***P≤0.001.

5.5. Auranofin, but Not Exogenously Supplied or Chemogenetically Produced H₂O₂, Significantly Enhances Nrf2 Levels Under Normoxic Conditions

The impact of H₂O₂ on Nrf2 levels was examined using multiple approaches. In the chemogenetic method (Figure 5.12), hCMEC/D3 cells expressing either cytosolic (Figure 5.12.A) or mitochondrial (Figure 5.12.B) mDAAO were exposed to D-alanine concentrations ranging from 5 to 100 mM for 24 hours. No activation of Nrf2 was

detected in any group, regardless of oxygen conditions (5 kPa or room air) or the subcellular localization of mDAAO.

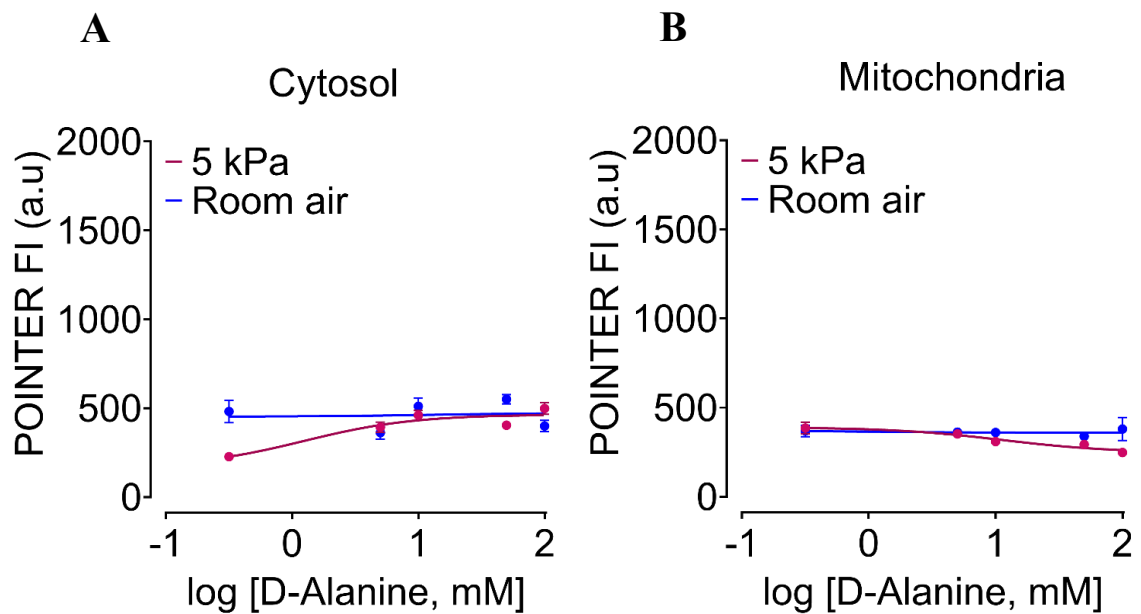


Figure 5.12. Evaluation of Nrf2 levels after 24 hours following chemogenetic H₂O₂ production in hCMEC/D3 cells. (A) POINTER responses in cytosolic mDAAO-expressing cells treated with D-alanine under room air and 5 kPa O₂. (B) POINTER responses in Mitochondrial mDAAO-expressing cells treated with D-alanine under the same conditions. All data points represent the mean±SEM of three biological replicates (N=3), each showing the mean of 12 snaps (n=12) and 5 cells were picked for analysis in each frame (n'=60).

In a separate experiment, cells were treated with 5 to 50 μ M of exogenous H₂O₂, and Nrf2 levels were quantified using POINTER intensity (Figure 5.13.A). A clear variation in Nrf2 response was observed between cells maintained in room air and those adapted to 5 kPa O₂. Significantly higher Nrf2 levels were found in all groups exposed to room air, compared to those cultured at 5 kPa. Specifically, at room air, both 30 μ M and 50 μ M H₂O₂ resulted in notable increases in Nrf2 levels, while only the highest concentration (50 μ M) induced a slight elevation at 5 kPa O₂ (Figure 5.13.A). These results indicate that Nrf2 activation under physiological oxygen conditions (5 kPa) is only triggered by supraphysiological concentrations of H₂O₂. Auranofin treatment, however, caused a pronounced increase in Nrf2 levels across all oxygen conditions (Figure 5.13.B). No significant differences in Nrf2 activation were found between cells adapted to room air or 5 kPa O₂. When the results of the different treatment strategies were compared,

Auranofin consistently produced the most substantial increase in Nrf2 levels, as shown by normalized data from cells grown in both oxygen environments (Figure 5.14).

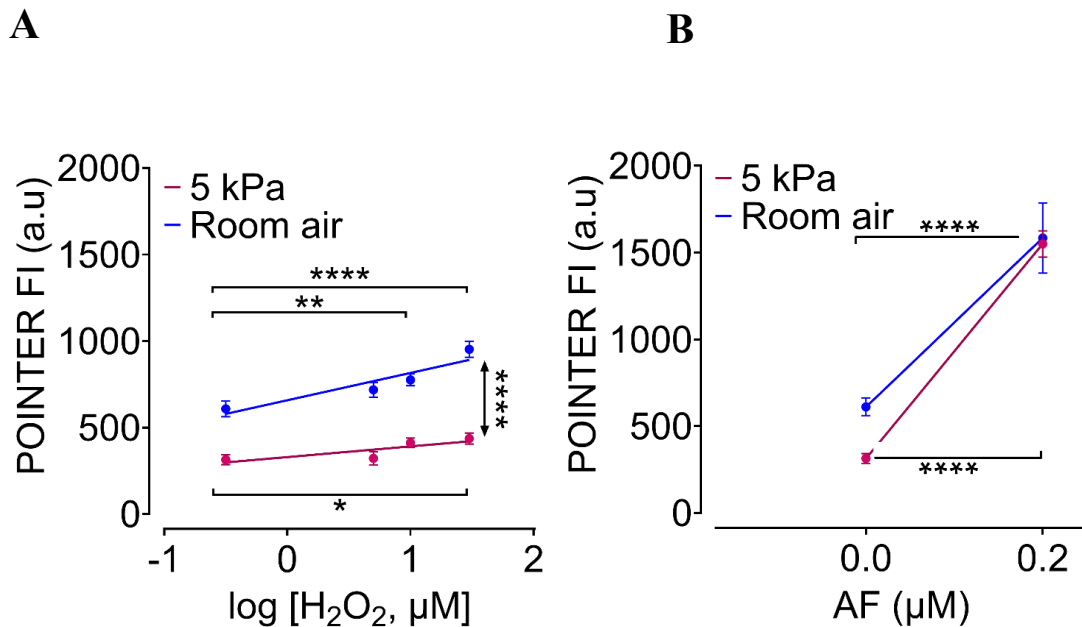


Figure 5.13. Nrf2 response to exogenous H₂O₂ and Auranofin. (A) hCMEC/D3 cells were treated with increasing concentrations of exogenous H₂O₂ (5–50 μM) under room air and 5 kPa O₂ conditions. Nrf2 levels were quantified using POINTER intensity. (B) Auranofin treatment significantly increased Nrf2 levels across both oxygen conditions, with no notable differences between room air and 5 kPa O₂. All data points represent the mean ±SEM of three biological replicates (N=3), each showing the mean of 12 snaps (n=12) and 5 cells were picked for analysis in each frame (n'=60). All statistical analysis were performed using one-way ANOVA with Tukey's multiple comparison post-test. **P≤0.01, ****P≤0.0001.

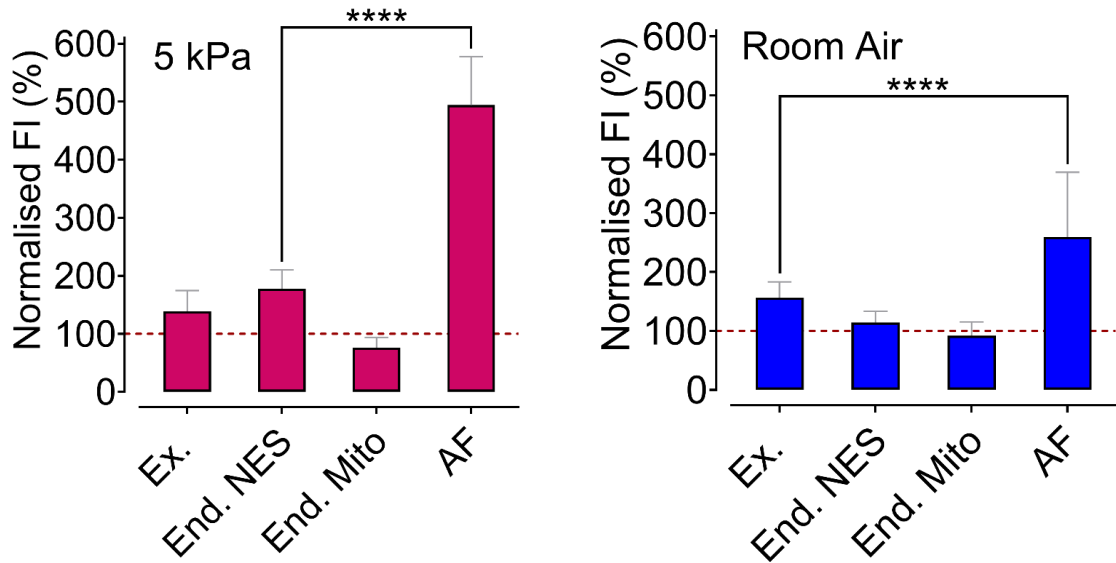


Figure 5.14. Comparative Nrf2 activation by different treatments. Auranofin demonstrated the most robust Nrf2 activation when normalized across cells adapted to 5 kPa O₂ (A) and room air (B), compared to exogenous or chemogenetic H₂O₂ treatments. All data points represent the mean \pm SEM of three biological replicates (N=3), each showing the mean of 12 snaps (n=12) and 5 cells were picked for analysis in each frame (n'=60). All statistical analysis were performed using one-way ANOVA with Tukey's multiple comparison post-test. ****P \leq 0.0001.

6. DISCUSSION

The relationship between oxidative stress, H_2O_2 as a second messenger, and Nrf2 dynamics is central to cellular defense mechanisms. Nrf2 is a critical transcription factor that regulates the expression of a wide array of cytoprotective genes involved in antioxidant responses, detoxification, and inflammation. Dysregulation of Nrf2 has been implicated in various diseases, including cancer, neurodegenerative disorders, and chronic inflammatory conditions (Kensler et al., 2007; Sies et al., 2017). Therefore, elucidating the mechanisms governing Nrf2 activation and the role of H_2O_2 as a signaling molecule in these pathways is of paramount importance, especially for the development of therapeutic strategies targeting diseases associated with oxidative stress.

Despite extensive research efforts aimed at understanding the nuances of Nrf2 activation, the intricate relationship between H_2O_2 and Nrf2 remains poorly understood, particularly under physiological oxygen conditions (5 kPa). Many studies tend to focus on room air conditions (18% O_2), which do not accurately reflect *in vivo* environments, leading to potentially misleading conclusions about cellular redox homeostasis (Altun et al., 2024; Jordan et al., 2024). Thus, our study aims to bridge this gap by developing POINTER, a novel oxygen-independent biosensor, to monitor Nrf2 levels under physiological oxygen conditions. This innovative tool facilitates more accurate insights into Nrf2 dynamics by circumventing the common issue of fluorescence-based reporters that rely on oxygen for chromophore maturation—an inherent limitation in traditional fluorescent-based, like GFP-based, systems (Liang *et al.*, 2022).

To validate POINTER, we utilized hCMEC/D3 cells, which are known for their resistance to transient transfection (Altun *et al.*, 2024; Eroğlu, 2022). Given their

physiological relevance in the blood-brain barrier and susceptibility to oxidative stress, hCMEC/D3 cells provided an ideal model system. To address the challenges associated with transfection, we employed lentiviral transfection methods, generating a stable cell line capable of consistently expressing the POINTER biosensor. Our results confirmed that cells cultured under physiological normoxia exhibited lower Nrf2 levels compared to those cultured in room air, aligning with previous research emphasizing the role of pericellular oxygen in modulating redox signaling (Chapple *et al.*, 2016; Warpsinski *et al.*, 2020).

The implications of these findings are profound. Nrf2 is traditionally thought to be activated by oxidative stress, but our results suggest that oxygen levels may critically modulate Nrf2 levels independent of oxidative stress. This insight prompts a reevaluation of the prevailing assumptions regarding Nrf2 dynamics, particularly in the context of chronic diseases characterized by persistent oxidative stress.

The importance of oxygen tension in regulating Nrf2 activation cannot be overstated. Previous studies have demonstrated that cells adapted to physiological oxygen conditions display reduced Nrf2 activity, despite evidence of nuclear accumulation (Chapple *et al.*, 2016; Maddalena *et al.*, 2017). For example, in ischemic stroke models, researchers found that redox defenses and Nrf2 activation are highly sensitive to oxygen levels, with diminished responses observed under physiological conditions (Warpsinski *et al.*, 2020). This phenomenon raises the question: why does physiological oxygen tension appear to attenuate Nrf2 activation? One potential explanation is that elevated oxygen levels promote the rapid degradation of ROS, thus limiting their ability to activate redox-sensitive pathways, including the Nrf2-Keap1 axis. The Keap1 protein functions as a negative regulator of Nrf2, sequestering it in the cytoplasm and facilitating its ubiquitination and degradation under normal conditions. Under oxidative stress, modifications to Keap1 can inhibit its interaction with Nrf2, allowing Nrf2 to translocate to the nucleus and activate target genes (Kensler *et al.*, 2007).

In our study, we sought to explore the effects of intracellular H₂O₂ manipulation on Nrf2 activation using three distinct methods: exogenous H₂O₂ application, chemogenetic production via the mDAAO enzyme, and pharmacological induction through Auranofin. Each method provided unique insights into how oxidative stress modulates Nrf2 levels. Interestingly, the administration of exogenous H₂O₂ resulted in increased Nrf2 levels potentially only under room air conditions. This observation suggests that while high doses of H₂O₂ can act as a signaling molecule capable of activating Nrf2, its effectiveness may

be limited by oxygen tension. High concentrations of H₂O₂ lead to a rapid influx of ROS that can overwhelm cellular antioxidant defenses, resulting in cellular damage and apoptosis. Conversely, under physiological oxygen levels, the immediate degradation of H₂O₂ may prevent its accumulation and subsequent Nrf2 activation.

This finding aligns with previous research that underscores the complexities of ROS signaling. While low to moderate levels of H₂O₂ can activate Nrf2, excessive concentrations may lead to cellular dysfunction and promote pro-apoptotic signaling pathways (Sinenko et al., 2021; Zhou et al., 2022). Thus, the relationship between H₂O₂ concentration and Nrf2 activation is not linear, but rather characterized by a delicate balance between oxidative stress and cellular homeostasis.

The chemogenetic approach, utilizing the mDAAO enzyme to produce H₂O₂, revealed a different narrative. Despite sustained H₂O₂ production that persisted even after 24 hours, we observed no increase in Nrf2 levels under both physiological normoxia (5 kPa) and room air conditions. This lack of response raises important questions regarding the signaling pathways activated by continuous, low-level H₂O₂ production.

It is conceivable that prolonged exposure to low-level H₂O₂ may induce a state of adaptation in endothelial cells, whereby antioxidant defenses are upregulated to mitigate oxidative stress. This concept is supported by findings in chronic conditions like COPD, where the sustained presence of ROS leads to impaired Nrf2 activation despite high levels of oxidative stress (Malhotra et al., 2009). The chemogenetic approach may therefore promote adaptation through enhancement of the antioxidant system rather than direct Nrf2 activation.

In contrast, Auranofin, a potent inhibitor of TrxR, consistently activated Nrf2 under both physiological normoxia and room air conditions. Auranofin disrupts the cellular antioxidant defense by inhibiting TrxR, leading to an accumulation of H₂O₂ and triggering the Nrf2 pathway as a defensive mechanism (Casini and Messori, 2011; Radenkovic et al., 2017). This finding suggests that the inhibition of antioxidant defenses, rather than direct oxidative stress, may be crucial for robust Nrf2 activation.

The literature overwhelmingly supports the notion that H₂O₂ activates Nrf2 (Bell et al., 2011; Fourquet et al., 2010; Kanner, 2020). However, the complexities of this relationship are illustrated by discrepancies in the field. For example, studies by Haskew-Layton et al. (Haskew-Layton et al., 2010) indicated that low levels of H₂O₂ produced enzymatically in astrocytes conferred neuroprotection through mechanisms independent of Nrf2 activation. In contrast, Bell et al. (Bell *et al.*, 2011) argued that mild oxidative

stress, including subtoxic doses of H₂O₂, robustly activates Nrf2, thereby enhancing neuroprotection.

This divergence in findings underscores the critical impact of H₂O₂ concentration and delivery method on the resulting cellular pathways and protective mechanisms. Haskew-Layton et al. emphasized methodological differences, noting that their use of controlled enzymatic production of H₂O₂ differed from Bell et al.'s direct addition of H₂O₂ at subtoxic levels, potentially leading to varying outcomes in Nrf2 activation (Haskew-Layton et al., 2011).

Furthermore, a recent study by Jose et al. (Jose et al., 2024) revealed that the activation of transcription factors such as Nrf2 by H₂O₂ is both dose-dependent and temporally coordinated. This research highlights that Nrf2 activation occurs in response to low H₂O₂ levels, whereas acute high concentrations of H₂O₂ may not activate Nrf2 but instead activate other transcription factors such as FOXO1, NF-κB, and NFAT1. The coordinated shift at high levels of H₂O₂ illustrates the temporal regulation of Nrf2 activity.

One of the major limitations of current research on Nrf2 and H₂O₂ dynamics is the failure to account for physiologically relevant oxygen conditions. Most studies are conducted in room air, which does not accurately reflect the *in vivo* environment and can lead to erroneous conclusions regarding redox signaling pathways. Our study emphasizes the importance of pericellular oxygen in modulating oxidative stress responses and highlights the need for future research to incorporate physiologically relevant oxygen levels (Altun *et al.*, 2024; Purdom-Dickinson et al., 2007).

Moreover, while our study provides valuable insights into Nrf2 activation under different oxidative stress conditions, it also raises several questions. For instance, why does the chemogenetic approach fail to activate Nrf2 despite robust H₂O₂ production? Could this be due to enhanced antioxidant capacity in cells adapted to physiological oxygen, or are other pathways involved in modulating Nrf2 activation under these conditions? Addressing these questions will be critical for understanding the complexities of Nrf2 regulation and its implications for disease pathology.

Another important avenue for future research is to explore the therapeutic potential of manipulating Nrf2 pathways in various diseases characterized by oxidative stress. Given the role of Nrf2 in cytoprotection and cellular resilience, understanding the specific contexts in which Nrf2 can be activated or inhibited could lead to novel strategies for treating conditions like neurodegenerative diseases, cancer, and metabolic disorders.

Furthermore, investigating the interplay between Nrf2 activation, antioxidant responses, and other redox-sensitive transcription factors could reveal intricate networks that govern cellular responses to stress.

As our understanding of Nrf2 dynamics continues to evolve, it is crucial to adopt a comprehensive approach that considers the multifaceted roles of H₂O₂ and oxygen levels in modulating redox signaling pathways. This study sets the stage for further investigations into the therapeutic implications of targeting Nrf2 in oxidative stress-related diseases, ultimately contributing to the advancement of novel therapeutic strategies.

7. CONCLUSION

To summarize, this study presents POINTER, a new oxygen-independent biosensor developed to monitor Nrf2 levels in human cerebral microvascular endothelial cells. The biosensor was validated across different oxygen conditions, revealing that cells grown in physiological normoxia (5 kPa) displayed higher Nrf2 levels than those in room air. This highlights the sensor's effectiveness in detecting oxygen-related changes in Nrf2 activity. Several methods were tested to generate H₂O₂ — exogenous administration, chemogenetic production, and pharmacological induction using Auranofin — to assess their effects on Nrf2 activation. While exogenous H₂O₂ elevated Nrf2 at high concentrations in room air, the chemogenetic method had no significant effect regardless of oxygen levels. Auranofin, however, increased Nrf2 levels under both oxygen conditions, emphasizing the role of inhibiting antioxidant mechanisms and accumulating H₂O₂ for significant Nrf2 activation in cells adapted to physiological oxygen. These findings offer deeper insights into the pathways of Nrf2 activation by H₂O₂, especially in the context of oxidative stress responses in hCMEC/D3 cells. Most importantly, POINTER has proven to be a reliable Nrf2 biosensor across various oxygen environments, making it a useful tool for drug screening and Nrf2-related disease studies.

8. BIBLIOGRAPHY

- Abdalbari, F.H., and Telleria, C.M. (2021). The gold complex auranofin: new perspectives for cancer therapy. *Discover Oncology* 12, 42.
- Ahmad, T., Iqbal, A., Halim, S.A., Uddin, J., Khan, A., El Deeb, S., and Al-Harrasi, A. (2022). Recent advances in electrochemical sensing of hydrogen peroxide (H₂O₂) released from cancer cells. *Nanomaterials* 12, 1475.
- Al-Mubarak, B.R., Bell, K.F., Chowdhry, S., Meakin, P.J., Baxter, P.S., McKay, S., Dando, O., Ashford, M.L., Gazaryan, I., and Hayes, J.D. (2021). Non-canonical Keap1-independent activation of Nrf2 in astrocytes by mild oxidative stress. *Redox biology* 47, 102158.
- Alim, I., Haskew-Layton, R.E., Aleyasin, H., Guo, H., and Ratan, R.R. (2014). Spatial, temporal, and quantitative manipulation of intracellular hydrogen peroxide in cultured cells. In *Methods in enzymology*, (Elsevier), pp. 251-273.
- Altun, H.Y., Secilmis, M., Yang, F., Caglar, T.A., Vatandaslar, E., Toy, M.F., Vilain, S., Mann, G.E., Öztürk, G., and Eroglu, E. (2024). Visualizing hydrogen peroxide and nitric oxide dynamics in endothelial cells using multispectral imaging under controlled oxygen conditions. *Free Radical Biology and Medicine* 221, 89-97.
- Aon, M.A., Stanley, B.A., Sivakumaran, V., Kembro, J.M., O'Rourke, B., Paolocci, N., and Cortassa, S. (2012). Glutathione/thioredoxin systems modulate mitochondrial H₂O₂ emission: an experimental-computational study. *Journal of General Physiology* 139, 479-491.
- Baird, L., Swift, S., Llères, D., and Dinkova-Kostova, A.T. (2014). Monitoring Keap1–Nrf2 interactions in single live cells. *Biotechnology advances* 32, 1133-1144.

- Becker, K., Gromer, S., Schirmer, R.H., and Müller, S. (2000). Thioredoxin reductase as a pathophysiological factor and drug target. *European journal of biochemistry* 267, 6118-6125.
- Bell, K.F., Al-Mubarak, B., Fowler, J.H., Baxter, P.S., Gupta, K., Tsujita, T., Chowdhry, S., Patani, R., Chandran, S., and Horsburgh, K. (2011). Mild oxidative stress activates Nrf2 in astrocytes, which contributes to neuroprotective ischemic preconditioning. *Proceedings of the National Academy of Sciences* 108, E1-E2.
- Bozem, M., Knapp, P., Mirčeski, V., Slowik, E.J., Bogeski, I., Kappl, R., Heinemann, C., and Hoth, M. (2018). Electrochemical quantification of extracellular local H₂O₂ kinetics originating from single cells. *Antioxidants & redox signaling* 29, 501-517.
- Bruns, D.R., Drake, J.C., Biela, L.M., Peelor III, F.F., Miller, B.F., and Hamilton, K.L. (2015). Nrf2 signaling and the slowed aging phenotype: Evidence from long-lived models. *Oxidative medicine and cellular longevity* 2015, 732596.
- Calabrese, E.J., and Kozumbo, W.J. (2021). The phytoprotective agent sulforaphane prevents inflammatory degenerative diseases and age-related pathologies via Nrf2-mediated hormesis. *Pharmacological research* 163, 105283.
- Caltabiano, M.M., Poste, G., and Greig, R.G. (1988). Induction of the 32-kD human stress protein by auranofin and related triethylphosphine gold analogs. *Biochemical pharmacology* 37, 4089-4093.
- Carl, S.M., Lindley, D.J., Das, D., Couraud, P.O., Weksler, B.B., Romero, I., Mowery, S.A., and Knipp, G.T. (2010). ABC and SLC transporter expression and proton oligopeptide transporter (POT) mediated permeation across the human blood-brain barrier cell line, hCMEC/D3 [corrected]. *Molecular pharmaceutics* 7, 1057-1068.
- Casini, A., and Messori, L. (2011). Molecular mechanisms and proposed targets for selected anticancer gold compounds. *Current topics in medicinal chemistry* 11, 2647-2660.
- Chapple, S.J., Keeley, T.P., Mastronicola, D., Arno, M., Vizcay-Barrena, G., Fleck, R., Siow, R.C., and Mann, G.E. (2016). Bach1 differentially regulates distinct Nrf2-dependent genes in human venous and coronary artery endothelial cells adapted to physiological oxygen levels. *Free Radical Biology and Medicine* 92, 152-162.
- Chen, B., Longtine, M.S., and Nelson, D.M. (2013). Pericellular oxygen concentration of cultured primary human trophoblasts. *Placenta* 34, 106-109.

- Chen, B., Lu, Y., Chen, Y., and Cheng, J. (2015). The role of Nrf2 in oxidative stress-induced endothelial injuries. *J Endocrinol* 225, R83-99.
- Cochemé, H.M., Quin, C., McQuaker, S.J., Cabreiro, F., Logan, A., Prime, T.A., Abakumova, I., Patel, J.V., Fearnley, I.M., and James, A.M. (2011). Measurement of H₂O₂ within living *Drosophila* during aging using a ratiometric mass spectrometry probe targeted to the mitochondrial matrix. *Cell metabolism* 13, 340-350.
- Cox, A.G., Brown, K.K., Arner, E.S., and Hampton, M.B. (2008). The thioredoxin reductase inhibitor auranofin triggers apoptosis through a Bax/Bak-dependent process that involves peroxiredoxin 3 oxidation. *Biochemical pharmacology* 76, 1097-1109.
- Cuadrado, A. (2016). NRF2 in neurodegenerative diseases. *Current Opinion in Toxicology* 1, 46-53.
- Dmitriev, R.I., Zhdanov, A.V., Jasionek, G., and Papkovsky, D.B. (2012). Assessment of cellular oxygen gradients with a panel of phosphorescent oxygen-sensitive probes. *Analytical chemistry* 84, 2930-2938.
- Dodson, M., and Zhang, D.D. (2017). Non-canonical activation of NRF2: New insights and its relevance to disease. *Current pathobiology reports* 5, 171-176.
- Drechsel, D.A., and Patel, M. (2010). Respiration-dependent H₂O₂ removal in brain mitochondria via the thioredoxin/peroxiredoxin system. *Journal of Biological Chemistry* 285, 27850-27858.
- Ebbesen, P., Eckardt, K.-U., Ciampor, F., and Pettersen, E.O. (2004). Linking measured intercellular oxygen concentration to human cell functions. *Acta Oncologica* 43, 598-600.
- Egbujor, M.C., Olaniyan, O.T., Emeruwa, C.N., Saha, S., Saso, L., and Tucci, P. (2024). An insight into role of amino acids as antioxidants via NRF2 activation. *Amino Acids* 56, 23.
- Eroğlu, E. (2022). Simultaneous manipulation and imaging of chemogenetically induced hydrogen peroxide in hardly transfectable endothelial cells. *Cumhuriyet Science Journal*.
- Finkelstein, A., Walz, D., Batista, V., Mizraji, M., Roisman, F., and Misher, A. (1976). Auranofin. New oral gold compound for treatment of rheumatoid arthritis. *Annals of the rheumatic diseases* 35, 251-257.

- Fourquet, S., Guerois, R., Biard, D., and Toledano, M.B. (2010). Activation of NRF2 by nitrosative agents and H₂O₂ involves KEAP1 disulfide formation. *Journal of Biological Chemistry* 285, 8463-8471.
- Furst, D.E. (1983). Mechanism of action, pharmacology, clinical efficacy and side effects of auranofin: an orally administered organic gold compound for the treatment of rheumatoid arthritis. *Pharmacotherapy: The Journal of Human Pharmacology and Drug Therapy* 3, 284-296.
- Gallego-Selles, A., Martin-Rincon, M., Martinez-Canton, M., Perez-Valera, M., Martín-Rodríguez, S., Gelabert-Rebato, M., Santana, A., Morales-Alamo, D., Dorado, C., and Calbet, J.A. (2020). Regulation of Nrf2/Keap1 signalling in human skeletal muscle during exercise to exhaustion in normoxia, severe acute hypoxia and post-exercise ischaemia: Influence of metabolite accumulation and oxygenation. *Redox biology* 36, 101627.
- Gamberi, T., Chiappetta, G., Fiaschi, T., Modesti, A., Sorbi, F., and Magherini, F. (2022). Upgrade of an old drug: Auranofin in innovative cancer therapies to overcome drug resistance and to increase drug effectiveness. *Medicinal Research Reviews* 42, 1111-1146.
- Han, Y., Chen, P., Zhang, Y., Lu, W., Ding, W., Luo, Y., Wen, S., Xu, R., Liu, P., and Huang, P. (2019). Synergy between auranofin and celecoxib against colon cancer in vitro and in vivo through a novel redox-mediated mechanism. *Cancers* 11, 931.
- Hansen, M.C., Palmer Jr, R.J., Udsen, C., White, D.C., and Molin, S. (2001). Assessment of GFP fluorescence in cells of *Streptococcus gordonii* under conditions of low pH and low oxygen concentration. *Microbiology* 147, 1383-1391.
- Haskew-Layton, R.E., Ma, T.C., and Ratan, R.R. (2011). Reply to Bell et al.: Nrf2-dependent and-independent mechanisms of astrocytic neuroprotection. *Proceedings of the National Academy of Sciences* 108, E3-E4.
- Haskew-Layton, R.E., Payappilly, J.B., Smirnova, N.A., Ma, T.C., Chan, K.K., Murphy, T.H., Guo, H., Langley, B., Sultana, R., and Butterfield, D.A. (2010). Controlled enzymatic production of astrocytic hydrogen peroxide protects neurons from oxidative stress via an Nrf2-independent pathway. *Proceedings of the National Academy of Sciences* 107, 17385-17390.
- Hinkel, S., Mattern, K., Dietzel, A., Reichl, S., and Müller-Goymann, C. (2019). Parametric investigation of static and dynamic cell culture conditions and their impact on hCMEC/D3 barrier properties. *International journal of pharmaceutics* 566, 434-444.

- Howden, R. (2013). Nrf2 and cardiovascular defense. *Oxidative medicine and cellular longevity* 2013, 104308.
- Itoh, K., Wakabayashi, N., Katoh, Y., Ishii, T., Igarashi, K., Engel, J.D., and Yamamoto, M. (1999). Keap1 represses nuclear activation of antioxidant responsive elements by Nrf2 through binding to the amino-terminal Neh2 domain. *Genes & development* 13, 76-86.
- Jacobs, L.J., Hoehne, M.N., and Riemer, J. (2022). Measuring Intracellular H₂O₂ in Intact Human Cells Using the Genetically Encoded Fluorescent Sensor HyPer7. *Bio-protocol* 12, e4538-e4538.
- Johansson, K., Cebula, M., Rengby, O., Dreij, K., Carlström, K.E., Sigmundsson, K., Piehl, F., and Arnér, E.S. (2017). Cross talk in HEK293 cells between Nrf2, HIF, and NF-κB activities upon challenges with redox therapeutics characterized with single-cell resolution. *Antioxidants & redox signaling* 26, 229-246.
- Jordan, J.B., Smallwood, M.J., Smerdon, G.R., and Winyard, P.G. (2024). Cellular Pre-Adaptation to the High O₂ Concentration Used in Standard Cell Culture Confers Resistance to Subsequent H₂O₂-Induced Cell Death. *Antioxidants* 13, 269.
- Jose, E., March-Steinman, W., Wilson, B.A., Shanks, L., Parkinson, C., Alvarado-Cruz, I., Sweasy, J.B., and Paek, A.L. (2024). Temporal coordination of the transcription factor response to H₂O₂ stress. *Nature Communications* 15, 3440.
- Kaida, A., and Miura, M. (2012). Differential dependence on oxygen tension during the maturation process between monomeric Kusabira Orange 2 and monomeric Azami Green expressed in HeLa cells. *Biochemical and Biophysical Research Communications* 421, 855-859.
- Kanner, J. (2020). Polyphenols by generating H₂O₂, affect cell redox signaling, inhibit PTPs and activate Nrf2 axis for adaptation and cell surviving: in vitro, in vivo and human health. *Antioxidants* 9, 797.
- Karsa, M., Kosciolk, A., Bongers, A., Mariana, A., Failes, T., Gifford, A.J., Kees, U.R., Cheung, L.C., Kotecha, R.S., and Arndt, G.M. (2021). Exploiting the reactive oxygen species imbalance in high-risk paediatric acute lymphoblastic leukaemia through auranofin. *British Journal of Cancer* 125, 55-64.
- Kensler, T.W., Wakabayashi, N., and Biswal, S. (2007). Cell survival responses to environmental stresses via the Keap1-Nrf2-ARE pathway. *Annu. Rev. Pharmacol. Toxicol.* 47, 89-116.
- Kritsiligkou, P., Shen, T.K., and Dick, T.P. (2021). A comparison of Prx-and OxyR-

- based H₂O₂ probes expressed in *S. cerevisiae*. *Journal of Biological Chemistry* 297.
- Kwak, M.-K., and Kensler, T.W. (2010). Targeting NRF2 signaling for cancer chemoprevention. *Toxicology and applied pharmacology* 244, 66-76.
- Lakowicz, J.R., and Weber, G. (1973). Quenching of fluorescence by oxygen. Probe for structural fluctuations in macromolecules. *Biochemistry* 12, 4161-4170.
- Lewis, K.N., Mele, J., Hayes, J.D., and Buffenstein, R. (2010). Nrf2, a guardian of healthspan and gatekeeper of species longevity. *Integrative and comparative biology* 50, 829-843.
- Li, W., and Kong, A.N. (2009). Molecular mechanisms of Nrf2-mediated antioxidant response. *Molecular Carcinogenesis: Published in cooperation with the University of Texas MD Anderson Cancer Center* 48, 91-104.
- Liang, G.-T., Lai, C., Yue, Z., Zhang, H., Li, D., Chen, Z., Lu, X., Tao, L., Subach, F.V., and Piatkevich, K.D. (2022). Enhanced small green fluorescent proteins as a multisensing platform for biosensor development. *Frontiers in Bioengineering and Biotechnology* 10, 1039317.
- Liu, P., Dodson, M., Li, H., Schmidlin, C.J., Shakya, A., Wei, Y., Garcia, J.G., Chapman, E., Kiela, P.R., and Zhang, Q.-Y. (2021). Non-canonical NRF2 activation promotes a pro-diabetic shift in hepatic glucose metabolism. *Molecular Metabolism* 51, 101243.
- Lyublinskaya, O., and Antunes, F. (2019). Measuring intracellular concentration of hydrogen peroxide with the use of genetically encoded H₂O₂ biosensor HyPer. *Redox biology* 24, 101200.
- Ma, Q. (2013). Role of nrf2 in oxidative stress and toxicity. *Annual review of pharmacology and toxicology* 53, 401-426.
- Maddalena, L.A., Selim, S.M., Fonseca, J., Messner, H., McGowan, S., and Stuart, J.A. (2017). Hydrogen peroxide production is affected by oxygen levels in mammalian cell culture. *Biochemical and biophysical research communications* 493, 246-251.
- Malhotra, D., Thimmulappa, R., Vij, N., Navas-Acien, A., Sussan, T., Merali, S., Zhang, L., Kelsen, S.G., Myers, A., and Wise, R. (2009). Heightened endoplasmic reticulum stress in the lungs of patients with chronic obstructive pulmonary disease: the role of Nrf2-regulated proteasomal activity. *American journal of respiratory and critical care medicine* 180, 1196-1207.

- Martinez, C.-A., Cistulli, P.A., and Cook, K.M. (2019). A cell culture model that mimics physiological tissue oxygenation using oxygen-permeable membranes. *Bio-protocol* 9, e3371-e3371.
- Matzinger, M., Fischhuber, K., and Heiss, E.H. (2018). Activation of Nrf2 signaling by natural products-can it alleviate diabetes? *Biotechnology advances* 36, 1738-1767.
- Miri, S.M., Ouf, B.N.A., Çimen, Ş., Barakat, S., Zaki, A.G., Armouch, J., Vatandaşlar, E., Öztürk, G., and Eroglu, E. (2024). Visualizing the H₂O₂-Nrf2 Relationship Using an Oxygen-Independent Nrf2 Biosensor Under Controlled Oxygen Conditions. *Authorea Preprints*.
- Mukherjee, A., Weyant, K.B., Agrawal, U., Walker, J., Cann, I.K., and Schroeder, C.M. (2015). Engineering and characterization of new LOV-based fluorescent proteins from *Chlamydomonas reinhardtii* and *Vaucheria frigida*. *ACS synthetic biology* 4, 371-377.
- Omata, Y., Folan, M., Shaw, M., Messer, R.L., Lockwood, P.E., Hobbs, D., Bouillaguet, S., Sano, H., Lewis, J.B., and Wataha, J.C. (2006). Sublethal concentrations of diverse gold compounds inhibit mammalian cytosolic thioredoxin reductase (TrxR1). *Toxicology in vitro* 20, 882-890.
- Onodera, T., Momose, I., and Kawada, M. (2019). Potential anticancer activity of auranofin. *Chemical and Pharmaceutical Bulletin* 67, 186-191.
- Pak, V.V., Ezeriņa, D., Lyublinskaya, O.G., Pedre, B., Tyurin-Kuzmin, P.A., Mishina, N.M., Thauvin, M., Young, D., Wahni, K., and Gache, S.A.M. (2020). Ultrasensitive genetically encoded indicator for hydrogen peroxide identifies roles for the oxidant in cell migration and mitochondrial function. *Cell metabolism* 31, 642-653. e646.
- Pavlacký, J., and Polak, J. (2020). Technical feasibility and physiological relevance of hypoxic cell culture models. *Frontiers in endocrinology* 11, 57.
- Poller, B., Gutmann, H., Krähenbühl, S., Weksler, B., Romero, I., Couraud, P.O., Tuffin, G., Drewe, J., and Huwyler, J. (2008). The human brain endothelial cell line hCMEC/D3 as a human blood-brain barrier model for drug transport studies. *Journal of neurochemistry* 107, 1358-1368.
- Purdom-Dickinson, S.E., Sheveleva, E.V., Sun, H., and Chen, Q.M. (2007). Translational control of nrf2 protein in activation of antioxidant response by oxidants. *Molecular pharmacology* 72, 1074-1081.

- Qiao, P., Sun, Y., Wang, Y., Lin, S., An, Y., Wang, L., Liu, J., Huang, Y., Yang, B., and Zhou, H. (2023). Activation of NRF2 signaling pathway delays the progression of Hyperuricemic nephropathy by reducing oxidative stress. *Antioxidants* 12, 1022.
- Radenkovic, F., Holland, O., Vanderlelie, J.J., and Perkins, A.V. (2017). Selective inhibition of endogenous antioxidants with Auranofin causes mitochondrial oxidative stress which can be countered by selenium supplementation. *Biochemical pharmacology* 146, 42-52.
- Ransy, C., Vaz, C., Lombès, A., and Bouillaud, F. (2020). Use of H₂O₂ to cause oxidative stress, the catalase issue. *International journal of molecular sciences* 21, 9149.
- Rhee, S.G., Chang, T.-S., Jeong, W., and Kang, D. (2010). Methods for detection and measurement of hydrogen peroxide inside and outside of cells. *Molecules and cells* 29, 539-549.
- Robledinos-Antón, N., Fernández-Ginés, R., Manda, G., and Cuadrado, A. (2019). Activators and inhibitors of NRF2: a review of their potential for clinical development. *Oxidative medicine and cellular longevity* 2019, 9372182.
- Ruiz, S., Pergola, P.E., Zager, R.A., and Vaziri, N.D. (2013). Targeting the transcription factor Nrf2 to ameliorate oxidative stress and inflammation in chronic kidney disease. *Kidney international* 83, 1029-1041.
- Saha, S., Buttari, B., Profumo, E., Tucci, P., and Saso, L. (2022). A perspective on Nrf2 signaling pathway for neuroinflammation: a potential therapeutic target in Alzheimer's and Parkinson's diseases. *Frontiers in cellular neuroscience* 15, 787258.
- Saravi, S.S.S., Eroglu, E., Waldeck-Weiermair, M., Sorrentino, A., Steinhorn, B., Belousov, V., and Michel, T. (2020). Differential endothelial signaling responses elicited by chemogenetic H₂O₂ synthesis. *Redox biology* 36, 101605.
- Seo, H.-A., and Lee, I.-K. (2013). The role of Nrf2: adipocyte differentiation, obesity, and insulin resistance. *Oxidative medicine and cellular longevity* 2013, 184598.
- Shen, T., Jiang, T., Long, M., Chen, J., Ren, D.-M., Wong, P.K., Chapman, E., Zhou, B., and Zhang, D.D. (2015). A curcumin derivative that inhibits vinyl carbamate-induced lung carcinogenesis via activation of the Nrf2 protective response. *Antioxidants & redox signaling* 23, 651-664.
- Sies, H. (2017). Hydrogen peroxide as a central redox signaling molecule in

physiological oxidative stress: Oxidative eustress. *Redox biology* 11, 613-619.

Sies, H., Berndt, C., and Jones, D.P. (2017). Oxidative stress. *Annual review of biochemistry* 86, 715-748.

Silva-Islas, C.A., and Maldonado, P.D. (2018). Canonical and non-canonical mechanisms of Nrf2 activation. *Pharmacological research* 134, 92-99.

Sinenko, S.A., Starkova, T.Y., Kuzmin, A.A., and Tomilin, A.N. (2021). Physiological signaling functions of reactive oxygen species in stem cells: from flies to man. *Frontiers in cell and developmental biology* 9, 714370.

Smolyarova, D.D., Podgorny, O.V., Bilan, D.S., and Belousov, V.V. (2022). A guide to genetically encoded tools for the study of H₂O₂. *The FEBS journal* 289, 5382-5395.

Sykiotis, G.P., and Bohmann, D. (2008). Keap1/Nrf2 signaling regulates oxidative stress tolerance and lifespan in *Drosophila*. *Developmental cell* 14, 76-85.

Thangamani, S., Maland, M., Mohammad, H., Pascuzzi, P.E., Avramova, L., Koehler, C.M., Hazbun, T.R., and Seleem, M.N. (2017). Repurposing approach identifies auranofin with broad spectrum antifungal activity that targets Mia40-Erv1 pathway. *Frontiers in cellular and infection microbiology* 7, 4.

Thomasz, L., Aran, M., Pizarro, R., Ibanez, J., Pisarev, M., Converso, D., Juvenal, G., and Krawiec, L. (2007). Inhibition of peroxidase and catalase activities and modulation of hydrogen peroxide level by inositol phosphoglycan-like compounds. *Hormone and metabolic research* 39, 14-19.

Tirtorahardjo, J.A., Jan, S., Schweizer, S.S., Rosario, S.A., Du, Y., Zhang, J.J., Morrisette, N.S., and Andrade, R.M. (2021). Auranofin Resistance in *Toxoplasma gondii* Decreases the Accumulation of Reactive Oxygen Species but Does Not Target Parasite Thioredoxin Reductase.

Tonelli, C., Chio, I.I.C., and Tuveson, D.A. (2018). Transcriptional regulation by Nrf2. *Antioxidants & redox signaling* 29, 1727-1745.

Warpsinski, G., Smith, M.J., Srivastava, S., Keeley, T.P., Siow, R.C., Fraser, P.A., and Mann, G.E. (2020). Nrf2-regulated redox signaling in brain endothelial cells adapted to physiological oxygen levels: consequences for sulforaphane mediated protection against hypoxia-reoxygenation. *Redox Biology* 37, 101708.

Weiszenstein, M., Pavlikova, N., Elkalaf, M., Halada, P., Seda, O., Trnka, J., Kovar, J.,

- and Polak, J. (2016). The effect of pericellular oxygen levels on proteomic profile and lipogenesis in 3T3-L1 differentiated preadipocytes cultured on gas-permeable cultureware. *PLoS One* 11, e0152382.
- Weksler, B., Romero, I.A., and Couraud, P.-O. (2013). The hCMEC/D3 cell line as a model of the human blood brain barrier. *Fluids and Barriers of the CNS* 10, 1-10.
- Weksler, B., Subileau, E., Perriere, N., Charneau, P., Holloway, K., Leveque, M., Tricoire-Leignel, H., Nicotra, A., Bourdoulous, S., and Turowski, P. (2005). Blood-brain barrier-specific properties of a human adult brain endothelial cell line. *The FASEB journal* 19, 1872-1874.
- Wymann, M.P., von Tscherner, V., Deranleau, D.A., and Baggiolini, M. (1987). Chemiluminescence detection of H₂O₂ produced by human neutrophils during the respiratory burst. *Analytical biochemistry* 165, 371-378.
- Yu, Y., Zhao, H., Lin, J., Li, Z., Tian, G., Yang, Y.Y., Yuan, P., and Ding, X. (2022). Repurposing non-antibiotic drugs Auranofin and Pentamidine in combination to combat multidrug-resistant gram-negative bacteria. *International Journal of Antimicrobial Agents* 59, 106582.
- Zachar, V., Duroux, M., Emmersen, J., Rasmussen, J.G., Pennisi, C.P., Yang, S., and Fink, T. (2011). Hypoxia and adipose-derived stem cell-based tissue regeneration and engineering. *Expert opinion on biological therapy* 11, 775-786.
- Zenin, V., Ivanova, J., Pugovkina, N., Shatrova, A., Aksenov, N., Tyuryaeva, I., Kirpichnikova, K., Kuneev, I., Zhuravlev, A., and Osyayeva, E. (2022). Resistance to H₂O₂-induced oxidative stress in human cells of different phenotypes. *Redox biology* 50, 102245.
- Zhou, Y., Zhen, Y., Wang, G., and Liu, B. (2022). Deconvoluting the complexity of reactive oxygen species (ROS) in neurodegenerative diseases. *Frontiers in Neuroanatomy* 16, 910427.

APPENDIX A

List of Chemicals

Chemical	Manufacturing Company
Ampicillin	Sigma Aldrich, USA
Auranofin	Sigma Aldrich, USA
Calcium chloride (CaCl₂)	neoFroxx, Germany
D (+) Glucose	neoFroxx, Germany
D-alanine	Alfa Aesar
Dimethyl sulfoxide (DMSO)	PAN-Biotech, Germany
Dulbecco's Modified Eagle Medium	Gibco, USA
Endothelial Cell Growth Medium	CURIO BIOTECH, Switzerland
Essential amino acids	PAN-Biotech, Germany
Ethanol	Merck, Germany
Fetal Bovine Serum (FBS)	Capricorn Scientific, Germany
Glycerol	neoFroxx, Germany
HEPES	neoFroxx, Germany
Hydrochloric acid (HCl)	Merck, Germany
Hydrogen peroxide (H₂O₂)	neoFroxx, Germany
Liquid Broth	neoFroxx, Germany
Magnesium chloride (MgCl₂)	neoFroxx, Germany
MEM vitamins	Sigma Aldrich, USA
Penicillin/Streptomycin	Santa Cruz Biotechnology, USA
Phosphate Buffered Saline	Gibco, USA
PolyJet	SignaGen Laboratories, USA
Potassium Chloride (KCl)	neoFroxx, Germany
Propidium Iodide (PI)	SignaGen Laboratories, USA
Serum-Free Phenol Red Free DMEM	neoFroxx, Germany
Sodium chloride (NaCl)	neoFroxx, Germany
Sodium hydroxide (NaOH)	neoFroxx, Germany
Trypsin-EDTA	Sigma Aldrich, USA

APPENDIX B

Equipments

Equipment	Manufacturing Company
Axio Observer. Z17	Zeiss, Germany
Balance	Ohaus, USA
Biosafety Hood	FASTER S.r.l., Italy
Cell Freezing Container	Mr. Frosty, USA
Colibri 7 Light Source	Zeiss, Germany
Filter Sets	Zeiss, Germany
Glass coverslips	Glaswarenfabrik Karl Hecht , Germany
Heat block	VWR, USA
Hemocytometer	Isolab, Germany
Nanodrop	Thermo Scientific, USA
Perfusion Chamber	NGFI, Austria
pH meter	HANNA, Italy
Plan-Apochromat 20x/0.8 M27	Zeiss, Germany
Plan-Apochromat 40x/1.4 Oil	Zeiss, Germany
Shaking incubator	Thermo Scientific, USA
Tabletop centrifuge	Thermo Scientific, USA
Tabletop centrifuge	GYROZEN, South Korea
ThermoCycler	BioRad, USA
Waterbath	Thermo Scientific, USA
Cell Sorter	BD Biosciences, USA
Cell Analyzer	BD Biosciences, USA

APPENDIX C

Molecular Biology Kits

Equipment	Manufacturing Company
Midi-prep DNA Isolation	Qiagen, Germany
Mii-prep DNA Isolation	New England Biolabs, Inc (NEB), USA
Gel Purification and PCR Clean-Up	New England Biolabs, Inc (NEB), USA
Total RNA Isolation Kit	Vezyme, China
SuperMix for qPCR	Vezyme, China
qPCR Master Mix	Vezyme, China